Name: Wang Zhi

Degree: M. Eng

Dept: Chemical & Environmental Engineering

Thesis Title: Redox Cycling of Mercury Mediated by Bromine / Iron: Environmental Implications.

Abstract

The special characteristics of mercury, such as, long range atmospheric transport, its transformation between species, biomagnification, and neurotoxin make it as a pollutant of global concern. The chemical processes take place in the atmosphere and water systems are closely linked the transformations of mercury. Therefore, the environmental implications by the redox cycling of mercury mediated by bromine and iron are well investigated in this study.

The second order rate constants at room temperature (20~23°C) for the $Hg^0_{(aq)}$-Br_2, $Hg^0_{(aq)}$- HOBr and $Hg^0_{(aq)}$-OBr^- are determined to be 0.196 ± 0.03 $M^{-1}s^{-1}$, 0.279 ± 0.02 $M^{-1}s^{-1}$ and 0.273 ± 0.04 $M^{-1}s^{-1}$, respectively. Such slow rate constants also mean that the important atmospheric "sink" for mercury is not caused by aqueous bromine, but gaseous bromine.

The backward reaction between aqueous elemental mercury and ferric iron was found to proceed extremely slowly with the second-order rate constant of 0.73 ± 0.29 $M^{-1}s^{-1}$. The forward reaction between divalent mercury and ferrous iron was found to be light-catalyzed. The enhancement of the forward reaction rate is achieved by three main factors, e. g. low pH value, high concentrations of the ferrous iron; the presence of short wavelengths (in the UV range of sunlight) and high light intensity catalyze the rate of the forward reaction.

Keywords: Redox, Mercury, Bromine, Iron.

REDOX CYCLING OF MERCURY MEDIATED BY BROMINE / IRON: ENVIRONMENTAL IMPLICATIONS

WANG ZHI

NATIONAL UNIVERSITY OF SINGAPORE

2003

REDOX CYCLING OF MERCRUY MEDIATED BY BROMINE / IRON: ENVIRONMENTAL IMPLICATIONS

WANG ZHI

(B. ENG., ZHEJIANG UNIVERSITY)

A THESIS SUBMITTED

FOR THE DEGREE OF MASTER OF ENGINEERING

DEPARTMENT OF CHEMICAL & ENVIRONMENTAL ENGINEERING

NATIONAL UNIVERSITY OF SINGAPORE

2003

ACKNOWLEDGEMENT

During the two years of studying at the Department of Chemical and Environmental Engineering of National University of Singapore, many people have helped me and taught me through my study. I would like to thank the individuals who deserve special thanks.

First, I would like to express my deepest appreciation to my academic supervisor, Dr. Simo Olavi Pehkonen, for his constant guidance, support, inspiration, encouragement and humor during my study at NUS. His endless help and enthusiastic direction is valuable for the research to succeed when difficulties were encountered at the beginning of this research. This thesis would not have been possible without his guidance and inspiration.

Also I would like to thank Goh Kaihui. She carried out some of the experiments described herein during her Final Year Project at NUS. In addition, I want to thank Madam Li Xiang for providing me analyzing the samples by ICP-MS and her generous friendship, and Susan, Chia Yiut Ching, who have provided me help in handling the laboratory stuff.

There is no word that can express my thanks to my parents and my family for their continuous support and encouragement, which are the most important factors for me to study here.

Finally I thank all the people in the department who have provided me help and friendship for the past two years. I would like to thank the Department of Chemical & Environmental Engineering for the pleasant and stimulating environment in which to work. The research scholarship provided by NUS is gratefully acknowledged.

TABLE OF CONTENTS

SUMMARY

Mercury is notorious among the global environmental pollutants, and it is emitted into the atmosphere from a number of natural as well as anthropogenic sources. During long range transport of mercury in the atmosphere, it undergoes a series of physical, chemical and eco-toxicological transformations before being transported back to the earth through dry and wet deposition. Such transformations of mercury are closely linked to a number of complex chemical reactions. Therefore, to understand the cycle of mercury in the environment and to evaluate this toxic element's characteristics in the environment, we must understand the reactions involving mercury that take place in the atmosphere and natural waters.

The first study is to investigate the kinetics of aqueous elemental mercury oxidized by aqueous bromine species (i.e., bromine, hypobromous acid, and hypobromite). The second order rate constants at room temperature (20~23^{0}C) for the Hg^0-Br_2, Hg^0-HOBr and Hg^0-OBr^- are determined to be $0.196 \pm 0.03\ M^{-1}s^{-1}$, $0.279 \pm 0.02\ M^{-1}s^{-1}$ and $0.273 \pm 0.04\ M^{-1}s^{-1}$, respectively. Such slow rate constants also mean that the important atmospheric "sink" for mercury is not caused by aqueous bromine, but most likely gaseous bromine.

The second study is to investigate the reaction between iron and mercury. The reverse reaction between elemental mercury and ferric iron was found to proceed extremely slowly. The second order rate constant for the Hg^0-Fe^{3+} reaction was found to be $0.73 \pm 0.29\ M^{-1}s^{-1}$. The reaction between divalent mercury and ferrous iron was found to be light-catalyzed. The enhancement of the forward reaction rate is achieved by three main factors. Firstly, low pH value, secondly, high concentrations of the ferrous iron; thirdly, the presence of short wavelengths (in the UV range of sunlight) and high light intensity catalyze the rate of the forward reaction.

LIST OF FIGURES

LIST OF TABLES

CHAPTER 1

INTRODUCTION

1.1 PHYSICAL AND CHEMICAL PROPERTIES OF MERCURY

Mercury has an atomic number of 80, an atomic mass of 200.59, with a specific gravity of 13.55 g/cm^3, a melting point of -39.8 ^{0}C and a boiling point of 357 ^{0}C. In the periodic table of elements, mercury is a Group IIB of transition metal with a closed shell electronic configuration ($5d^{10}6s^2$).

Compared with metals in the same group, mercury has some unusual physical and chemical properties that distinguish it from the other transition metals. For example, mercury is the only metal that is a liquid at normal room temperature and due to this, mercury exists in ambient air predominantly as individual mercury atoms. Compared to the noble metal Pt with an ionization potential of 207 kcal mole^{-1}, mercury has a relatively high first ionization potential of 241 kcal mole^{-1}. This characteristic can used to explain its existence in the atmosphere principally in the reduced form, although this medium is famous for its oxidizing properties. Moreover, the longest wavelength which the elemental mercury vapor absorbs radiation is 253.6 nm. But only solar radiation with wavelengths greater than 290 nm can penetrate into the lower atmosphere, therefore mercury will not undergo any direct photochemical activation processes in the troposphere and the predominant species of mercury in the atmosphere is elemental mercury. Other unique and/or technologically important physical and chemical properties include: high surface tension (Hg^0 does not wet glass), high specific gravity (13.55 kg/L at 20 ^{0}C), low electrical resistance, and a constant volume of expansion over the entire temperature range of its liquid state. Due to its many valuable and useful properties, its economic importance in commerce, industry, mining, metallurgy, manufacturing, medicine and dentistry increased rapidly during the industrial revolution of 1800s and 1900s.

Mercury is notorious among the global environmental pollutants. In contrast with most other heavy metals, mercury and many of its compounds behave differently in the environment due to their volatility and capability for methylation. Mercury can exist in a large number of different physical and chemical forms with a wide range of physical, chemical, and eco-toxicological properties and consequently with fundamental importance for the environmental behavior. The most important chemical forms known to occur in the environment are metallic mercury, inorganic mercury, and organic mercury. Metallic mercury, a shiny, silver-white metal that is a liquid at room temperature, has a high vapor pressure (18 mg/m^3 at 24 ^0C when saturated) and a relatively low solubility in water (about 60 µg/L; Clever et al., 1985) and oil (5-50 mg/L; Berlin, 1986). Inorganic mercury can be far more soluble and has a strong affinity for chlorine, sulfur, and oxygen, especially sulphur.

Compared to inorganic mercury, organic mercury compounds are strongly accumulated by living organisms. By far the most common organic mercury compound in the environment is methylmercury. The ability of methylmercury to bio-concentrate more than a million-fold in the aquatic food chain is the main reason for concern about emissions/mobilization of mercury to the biosphere. Conversions between these different forms provide the basis of mercury's complex distribution pattern on local, regional, and global scales.

1.2 SOURCES

Mercury is released into the atmosphere from many natural (Siegel and Siegel, 1984; Fitzgerald, 1986; Xiao et al., 1991b, Mason et al., 1994; Lindberg et al, 1995) and anthropogenic sources (Lindqvist et al., 1991; Ferrara et al., 1992; Pirrone et al., 1996; Carpi and Lindberg, 1997; Lacerda, 1997; Pirrone et al., 2000). Mercury is a naturally

occurring metal found throughout the environment with a ubiquitous distribution. Mercury enters the environment as a result of normal breakdown of minerals in rocks and soil from exposure to wind and water, and from volcanic activity. Mercury releases from natural sources have remained relatively constant in recent years, resulting in a continuous increase in environmental mercury.

Human activities have resulted in the release of a wide variety of both inorganic and organic forms of mercury since the start of the industrial age. Fuel combustion, waste incineration, electrical industry, chloro-alkaline industry, refining and processes are the most important sources of anthropogenic mercury into the atmosphere, fresh, and sea water on a worldwide basis. As a result, the continuous release of mercury has resulted in current levels that are three to six times higher than the estimated levels in the preindustrial-era atmosphere. Total input into the atmosphere has been estimated at up to 150,000 tons per years. Natural emission (from volcanoes, wind erosion, and soil degasification) account for two-thirds of the input, while man-made release (including coal and petroleum combustion) account for about one-third (Korringa and Hagel, 1974; National Academy of Sciences, 1978; Berlin, 1986, Pirrone et al., 2000).

1.3 TOXICITY

The current understanding of environmental mercury contamination began with the discovery that human beings as well as birds and animals had been poisoned by eating fish and shellfish that accumulated great quantities of alkyl merucry released into the bay from acetaldehyde and vinyl chloride plants first at Minamata and later at Niigata, Japan between 1950 and 1968 (D'Itri & D'Itri, 1977; Harada, 1982; Ellis, 1989; Mishima, 1992). The mammalian nervous system, kidney, brain and liver are extremely sensitive to mercury. Not only methylmercury, which is produced primarily

by bacteria and an enzyme called methylcobalamin, but also inorganic mercury compounds are very toxic to organisms.

Releases of mercury to the environment are usually in the form of elemental or inorganic divalent mercury. Mercury concentrations in air are usually low and of little direct concern. But when mercury enters water bodies, biological processes transform it to a highly toxic form, methylmercury, an organic form of mercury which accumulates in fish and animals that eat fish (Wood et al., 1968; Jensen and Jernelö v, 1969; Jugo, 1976; Beijer and Jernelöv, 1978; US EPA, 1984).

At high doses, mercury exposure can cause tremors, changes in vision, deafness, muscle incoordination, loss of sensation and difficulties in memory, permanent damage to the brain and kidney, and even death (Bidstrup, 1972; NIOSH, 1978; US EPA, March, 1999).

The developing fetus is very sensitive to the effects of mercury, and women of child-bearing age are the population of greatest concern. Children of women that have been exposed to relatively high levels of methylmercury during pregnancy have exhibited a variety of abnormalities, including delayed onset of walking and talking, and reduced neurological test scores. Children exposed to lower methylmercury concentrations in the womb have exhibited delays and deficits in learning ability (Rustam and Hamdi, 1974; WHO, 1987).

1.4 CHARACTERISTICS AND SPECIES OF MERCURY IN THE ATMOSPHERE

The four most important chemical species of mercury in the atmosphere are elemental mercury, divalent mercury, particulate mercury and methylmercury. Elemental mercury (Hg^0), which is reported to account for over 95% of the total mercury in the atmosphere (Bloom and Fitzgerald, 1988) has an average residence time of 0.5 ~ 2

years (Slemr at al., 1981; Fitzgerald et al., 1984; Lindqvist at al., 1985). Thus, it can be transported long distances and be deposited by precipitation at remote locations. Hg^0 is uniformly distributed in the troposphere, with concentrations ranging from 2.0 to 5.0 ng/m^3 (Schroeder et al., 1991). Divalent mercury (Hg^{2+}), with concentrations between 0.09 and 0.19 ng/m^3 (Brosset, 1987), tends to exist in atmospheric waters, either dissolved or adsorbed onto particles in droplets (Ross and Vermette, 1995) and has a much shorter lifetime in the atmosphere from several days to a few weeks (Lindqvist and Rodhe, 1985; Slemr et al., 1985). On the other hand, Lindberg and Stratton (1998) measured gaseous Hg^{2+} and found that it can attain about 3% of total gaseous mercury with background concentrations of ~ 1 - 4 ng/m^3 (Slemr and Langer, 1992). Particulate mercury usually is a minor constituent 0.3 ~ 0.9% of total gaseous mercury and is largely from anthropogenic origins (Brosset 1982; Slemr et al., 1985; Iverfeldt, 1991; Xiao et al. 1991a). Methylmercury (CH_3Hg^+), which is highly resistant to environmental degradation, has been reported at less than 3% of the total gaseous mercury, except at near emissions sources (Fitzgerald et al., 1991). Atmospheric mercury can undergo various physical and chemical transformations between these species before being deposited back to the ground. Atmospheric deposition is an important source of contamination, since elevated levels of mercury can be found in waters that are remote from anthropogenic emission sources.

1.5 ATMOSPHERIC MERCURY CYCLE

The atmospheric cycle of mercury is determined by natural and anthropogenic emissions, a complex atmospheric chemistry, and wet and dry deposition processes. Atmospheric chemistry and especially the deposition of mercury are strongly linked together with the speciation of mercury released into the atmosphere by different

sources. On a global scale, the atmospheric mercury cycle is dominated by elemental mercury vapor which distributes (partitions) between the gaseous, aqueous, and particulate phases, i.e., between air, rain and/or fog and/or cloudwater, and suspended particulate matter. However the emission speciation of mercury is determined by the source characteristics and consequently exhibits a large regional variability. The total tropospheric mercury budget depends on natural emissions, anthropogenic emissions, and re-emissions (Nriagu, 1994; Lindqvist et al, 1991; Nriagu and Pacyna, 1998; Pirrone et al., 1996, 2000; Ebinghaus et al., 1999). Anthropogenic and natural mercury emissions refer to the mobilization or the release of geologically bound mercury by human activities and natural biotic and abiotic processes, respectively. Re-emission of mercury is the mass transfer of mercury to the atmosphere by biotic or abiotic processes drawing on a pool of mercury that was deposited to the Earth's surface after initial mobilization by either anthropogenic or natural activities (Ebinghaus et al., 1998). The global total atmospheric emission of mercury has been estimated to be in the range of 5,000~15,000 t $year^{-1}$ (Lindqvist et al., 1991; Fitzgerald, 1996; Sukhenko and Vasiliev, 1996), with contribution from the industry of 40% of total (Pacyna and Pacyna, 1996; Pirrone et al., 1996), whereas natural sources and re-emissions present up to 60% of total. The deposition pathway is dominated by the flux of emitted Hg^{2+} compounds (formally known as reactive gaseous mercury or RGM), the oxidation of elemental mercury vapor to Hg^{2+}, and subsequent wet and/or dry deposition. Mercury species attached to particles can be removed from the atmosphere by precipitation or dry deposition (Expert Panel, 1994), but these fluxes are generally less important. It has been reported that approximately 200,000 tons of mercury have been deposited to soils by anthropogenic emission sources since 1890 (Expert Panel, 1994).

Once deposited, formation of volatile gaseous mercury, formation of highly toxic methylmercury, and its enrichment in organisms and nutritional chains, and finally a destruction (demethylation) of methylmercury are the main features of the biological cycle of mercury. The linkage between the atmosphere and biological cycles is manifested in the deposition of atmospheric mercury species. Figure 1.1 illustrates the most important processes in the emission and deposition cycle of mercury in the atmosphere.

1.6 MERCUY SPECIES AND CYCLE IN AQUEOUS SYSTEM

In aqueous solutions, ionic mercury can exist in monovalent [Hg^{+}, $5d^{10}6s^{1}$] or divalent [Hg^{2+}, $5d^{10}6s^{0}$] forms. Hg^{+} exists in the form of a dimer, Hg_2^{2+}, while Hg^{2+} acts as a soft acid and can form stable complexes with ligands, such as OH^{-}, Cl^{-}, Br^{-}, I^{-}, SO_3^{-} and CN^{-}. Redox reactions of mercury are important in determining the fate of Hg in aquatic systems. The total mercury concentration in a water body is partly controlled by direct deposition from the atmosphere of the oxidized form, Hg^{2+}, and by volatilization of the reduced form, Hg^{0} (Amyot et al., 2000; Lalonde et al., 2001). The loss of Hg from the water column is therefore enhanced by in situ Hg^{2+} reduction and decreased by Hg^{0} oxidation.

1.7 SPRINGTIME DEPOSITION OF MERCURY IN ARCTIC & SUB-ARCTIC

Schroeder et al (1998) has reported surprisingly rapid depletion of Hg^{0} from the atmospheric boundary layer during spring in the high-Arctic region at Alert, Canada. Subsequently, intensive research has been carried out and it was discovered that Hg^{0} depletion is widespread throughout the Arctic (Lindberg et al., 2002) and sub-Arctic (Poissant, 2001) and is concurring with the enhanced mercury deposition in surface

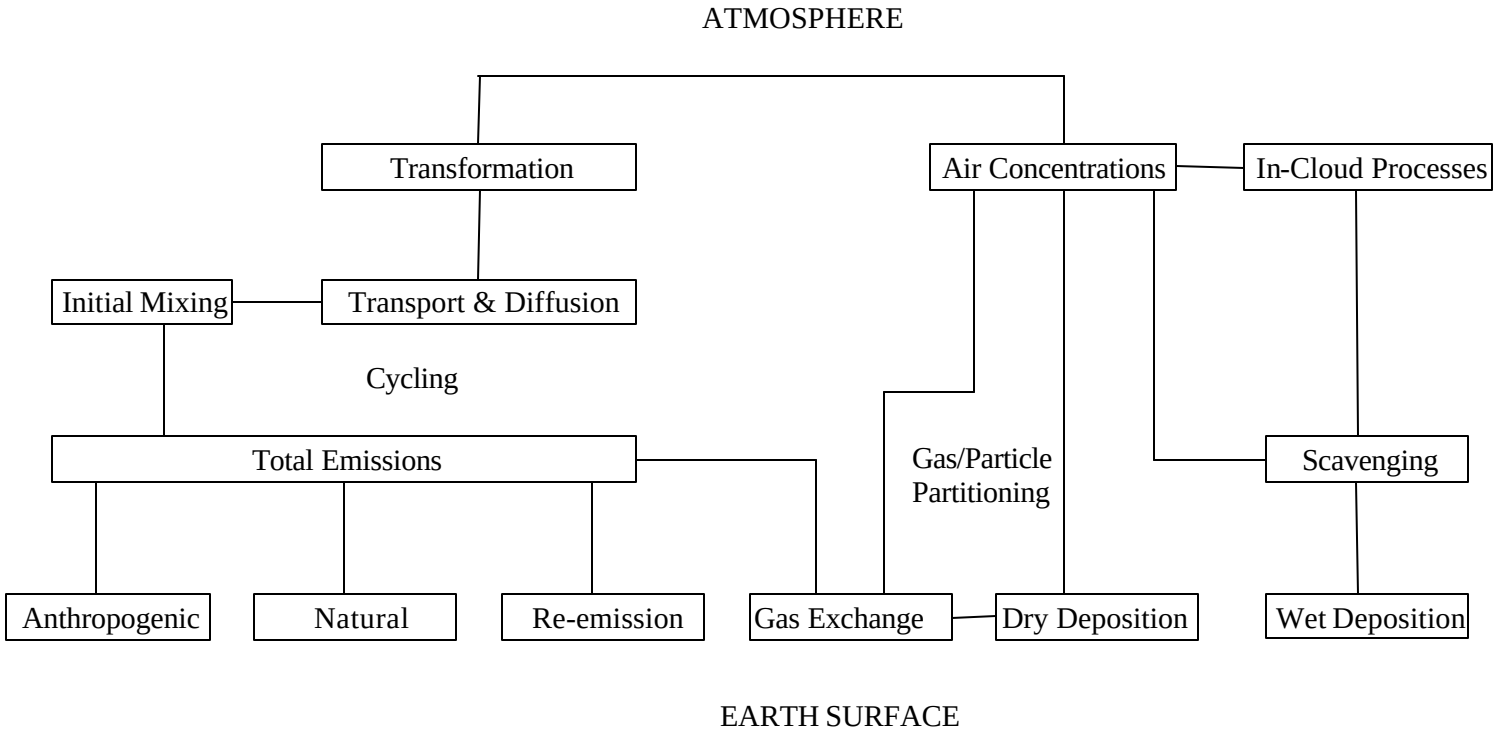

Adapted from Schroeder, W. H. and Lane. D.A., 1988

Figure 1.1 Mercury emission-to-deposition cycle in the atmosphere.

snow and ice (Lu et al., 2001). A chemical chain reaction begins with the first sunlight of spring, which causes components of vaporized sea-salt aerosols, namely bromine and chlorine, to convert into highly reactive species (Capozza, 2001). These airborne chemicals subsequently interact with elemental mercury vapor, ultimately causing the stable mercury to rapidly oxidize into soluble forms that easily deposit onto snow and ice surfaces (Capozza, 2001). Rapid depletions of atmospheric mercury (Hg^0) and ozone coinciding with high halogen concentrations have recently been observed in several high-Arctic and sub-Arctic regions (Schroeder et al., 1998; Ariya et al., 2002). Studies on the reactions of gaseous mercury with halogens indicate that atomic bromine is the only likely candidate to explain the rapid depletion of mercury in the Arctic (Ariya et al., 2002). But there is still a lack of information on the reactions that proceed in the aqueous phase. In the atmosphere, the aqueous reactions of mercury or mercury compounds can occur in rainwater, cloudwater, or fogwater and in the moisture associated with hygroscopic aerosols (Seigneur et al., 1994). For example, a water droplet can serve as a natural reactor as well as a storage medium for the chemical species involved in the reactions (Iverfeldt and Lindqvist, 1986; Brosset, 1987; Munthe and McElroy, 1992; Lin and Pehkonen, 1997).

1.8 ESSENTIAL RELATIONSHIP BETWEEN MERCURY AND IRON IN THE AQUEOUS SYSTEM

Several studies have suggested an interesting redox behavior between heavy metals and iron (Fendorf et al., 1996; Sedlak and Chan, 1997; Batchelor et al., 1998, Raposo et al., 2000; Zhang and Lindberg, 2001). Iron, being one of the most reactive and abundant elements in the aquatic environment, exists in two oxidation states, II and III, which are thermodynamically stable under anoxic and oxic conditions, respectively.

Ferric iron, Fe^{3+}, is photochemically reactive in aqueous media (Faust, 1994). Its role in mediating photochemical redox cycling of heavy metals in natural aqueous systems is well-established (Brezonik, 1994; Faust, 1994; Fendorf et al., 1996; Stumm and Morgan, 1996; Sedlak and Chen, 1997). Ferrous iron, Fe^{2+}, is abundant in many suboxic and anoxic soils and sediments (Anderson et al., 1994; Sedlak and Chen, 1997). Fe^{2+} also is produced through photochemical reactions that occur in sunlit natural waters (Voelker and Sedlak, 1995; McKnight et al., 1998; Waite and Morel, 1998). Moreover, it was shown that iron-organic complexes play a role in the redox cycling of mercury (Zhang and Lindberg, 2001). Since iron is abundant in most natural water systems at micromolar or higher levels, the redox coupling of these two elements is potentially very important for the biogeochemical cycling of mercury:

$Hg^{2+} + 2Fe^{2+} ? \quad Hg^{0} + 2Fe^{3+}$ (McCay and Anderson, 1921) (1.1)

CHAPTER 2

LITERATURE REVIEW

2.1 CHEMICAL TRANSFORMATIONS IN THE AQUEOUS PHASE

Chemical transformation of mercury in the atmospheric environment may take place in the gas phase or in the aqueous phase. Aqueous phase reactions can occur in cloud, fog and/or rainwater and in films of moisture associated with hygroscopic aerosols (Seigneur et al., 1994). Table 2.1 summarizes the reactions identified to be relevant in the aqueous phase chemistry of Hg. These reactions include the disproportionation of monovalent mercury into its elemental and divalent forms; the oxidation of elemental mercury to divalent mercury by ozone, hypochlorite ions, and some radicals; the reduction of divalent mercury to elemental mercury; and the complexation/dissociation of various mercuric species. Below is a review of published data on the reactions involving Hg^0 or Hg^{2+} species in the aqueous phase as well as reactions involving atomic and molecular halogens in the gas phase.

2.1.1 OXIDATION PATHWAYS

i) Oxidation of Hg^0 by ozone. This reaction can be described by the following equations (Weast, 1989).

$$Hg^0 \rightleftharpoons Hg^{2+} + 2e^- \qquad E^0 = -0.85\ V \qquad (2.1)$$

$$O_3 + H_2O + 2e^- \rightleftharpoons O_2 + 2OH^- \qquad E^0 = 1.24\ V \qquad (2.2)$$

$$O_3 + H_2O + Hg^0 \rightleftharpoons O_2 + 2OH^- + Hg^{2+} \qquad E^0 = 0.39\ V \qquad (2.3)$$

In solution, O_3 is a potent oxidant for elemental mercury under both acidic and alkaline conditions. Munthe (1992) has investigated the reaction of aqueous elemental mercury with ozone by using the relative rate technique. Sulfite was chosen as a reference reagent. The reaction was performed over the pH range of 4.5 ~ 9.5 and temperature varied from 278 to 308 K. Munthe (1992) found that the reaction rate constant of $(4.7 \pm 2.2) \times 10^7\ M^{-1}s^{-1}$ is independent of pH over the range of 5.2 ~ 6.2 and temperature.

Table 2.1 Summary of Aqueous-Phase Reactions of Mercury

No.	Reaction	Equilibrium or Rate Const.	Ref.
1	Hg_2^{2+} ? $Hg^0_{(aq)} + Hg^{2+}$	2.9×10^{-9} M	Lindqvst, O., 1991
2	$Hg^0_{(aq)} + O_{3(aq)}$? $Hg(II)_{(aq)} + O_{2(aq)}$	4.7×10^{7} $M^{-1}s^{-1}$	Munthe, 1992
3	$Hg^0_{(aq)} + HClO_{(aq)}$? $Hg^{2+} + Cl^- + OH^-$	(2.09 ± 0.06) x10^{7} $M^{-1}s^{-1}$	Lin and Pehkonen, 1998
4	$Hg^0_{(aq)} + ClO^-_{(aq)} + H^+$? $Hg^{2+} + Cl^- + OH^-$	(1.99 ± 0.065) x10^{7} $M^{-1}s^{-1}$	Lin and Pehkonen, 1998
5	$Hg_2^{2+} + H_2O_{2(aq)}$? $HgO_{(s)} + Hg^{2+} + H_2O_{(l)}$	6.0 $M^{-1}s^{-1}$	Munthe and McElroy, 1991
6	$Hg_2^{2+} + O_{3(aq)}$? Hg^{2+}	9.5×10^{6} $M^{-1}s^{-1}$	Iverfeldt et al., 1986; Lindqvst, O., 1991
7	$Hg(SO_3)_2^{2-}$? $Hg^0_{(aq)}$	1.0×10^{-4} s^{-1}	Lindqvst, O., 1991
8	$HgSO_{3(aq)} + SO_3^{2-}$? $Hg(SO_3)_2^{2-}$	2.5×10^{11} M^{-1}	Munthe et al., 1991
9	$Hg^{2+} + SO_3^{2-}$? $HgSO_{3(aq)}$	5.0×10^{12} M^{-1}	Munthe et al. 1991
10	$HgSO_{3(aq)}$? $Hg^0_{(aq)} + SO_4^{2-}$	0.6 s^{-1}	Munthe et al. 1991
11	$HgCl_{2(aq)} \xrightarrow{h\nu} Hg^{2+}_{(aq)} + 2Cl^-$	Not available	Lindqvist, O., 1991
12	$Hg(OH)_{2(aq)} \xrightarrow{h\nu} Hg^0_{(aq)}$	3. x10^{-7} s^{-1}	Xiao et al., 1994
13	$HgCl_{2(s)}$? $HgCl_{2(aq)}$	0.27 M	Sillén et al., 1964
14	$HgCl_{2(aq)}$? $Hg^{2+} + 2Cl^-$	10^{-14} M^2	Sillén et al., 1964
15	$HgCl_{2(aq)} + 2Cl^-$? $HgCl_4$	70.8 M^{-2}	Sillén et al., 1964
16	$Hg(OH)_{2(s)}$? $Hg(OH)_{2(aq)}$	3.5×10^{-4} M	Sillén et al., 1964
17	$Hg(OH)_{2(aq)}$? $Hg^{2+} + 2OH^-$	10^{-22} M^2	Sillén et al., 1964

At high pH values, the consummation rate of ozone by sulfite is faster than by mercury. Thus, no decrease in the concentration of Hg^0 could be measured after adding a small amount of O_3.

Pleijel and Munthe (1995) suggested the reaction mechanism is as follows:

$$Hg^0_{(aq)} + O_{3(aq)} \xrightarrow{H^+} Hg^{2+}_{(aq)} + OH^- + O_{2(aq)} \qquad (2.4)$$

ii) Oxidation by H_2O_2. The oxidation reaction can be represented by the following equations (Weast, 1989).

Hg_2^{2+} ? $2Hg^{2+} + 2e^-$ $E^0 = -0.92$ V (2.5)

$H_2O_2 + 2H^+ + 2e^-$? $2H_2O$ $E^0 = 1.78$ V (2.6)

$Hg^0 + H_2O_2 + 2H^+$? $Hg^{2+} + 2H_2O$ $E^0 = 0.86$ V (2.7)

Several investigators have suggested that oxidation of Hg^0 by H_2O_2 may be important in the atmospheric environment (Lindqvist et at., 1984; Brosset, 1987; Kobayashi, 1987; Schroeder 1991). But Kobayashi (1987) reported that H_2O_2 did not oxidize elemental mercury in the absence of ferric ions. Munthe and McElroy (1991) later reinvestigated this reaction and could not observe any oxidation of Hg_2^{2+} by H_2O_2 with or without Fe^{3+} present. But when in the presence of ferrous ion, an obvious concentration decrease of the Hg_2^{2+} was detected. Stopped-flow techniques and monovalent mercury were used for this oxidation reactions and the upper limit of the rate constants were estimated assuming second-order kinetics and a maximum depletion of mercury species of 1% in 10 s with the value of 6.0 $M^{-1}s^{-1}$. The mechanistic scheme of the reaction suggested by Munthe and McElroy (1991) is shown below.

$Hg_2^{2+} + H_2O_{2(aq)}$? $HgO_{(s)} + Hg^{2+} + H_2O_{(l)}$ (2.8)

iii) Oxidation by hypochlorous acid. The following electrochemical equations illustrate the electical potential of the reactions between aqueous elemental mercury and hypochlorous acid and/or hypochlorite.

Hg^0 ? $Hg^{2+} + 2e^-$ $E^0 = -0.85$ V (2.9)

$HClO + 2e^- + H^+$? $Cl^- + H_2O$ $E^0 = 1.495$ V (2.10)

$Hg^0 + HClO + H^+$? $Hg^{2+} + Cl^- + H_2O$ $E^0 = 0.645$ V (2.11)

And

$Hg^0 \rightarrow Hg^{2+} + 2e^-$ $E^0 = -0.85$ V (2.12)

$ClO^- + 2e^- + H^+ \rightarrow Cl^- + OH^-$ $E^0 = 1.36$ V (2.13)

$Hg^0 + ClO^- + H^+ \rightarrow Hg^{2+} + Cl^- + OH^-$ $E^0 = 0.51$ V (2.14)

Kobayashi (1987) studied the aqueous phase oxidation of Hg^0 by bubbling Hg vapor into solutions of HOCl and ClO^- over the pH range of 1.2 to 8.1. The reaction rate (Hg dissolution and/or oxidation) was reported to be sufficiently fast and independent of the ClO^- concentration (Kobayashi, 1987). Lin and Pehkonen (1998) re-measured this reaction by using chloramines as the free chlorine reservoir, maintaining the concentration of chlorine at ~ 10^{-10} M in the solution. The rate constants for the reaction of Hg^0 - HOCl and Hg^0 - OCl^- were reported to be (2.09 ± 0.06) x 10^6 $M^{-1}s^{-1}$ and (1.99 ± 0.05) x 10^6 $M^{-1}s^{-1}$, respectively.

The mechanistic scheme of the reaction suggested by Lin and Pehkonen (1998) is shown below.

$Hg^0_{(aq)} + HOCl_{(aq)} \rightarrow Hg^{2+}_{(aq)} + Cl^-_{(aq)} + OH^-_{(aq)}$ (2.15)

$OCl^- + Hg^0_{(aq)} \xrightarrow{H^+} Hg^{2+}_{(aq)} + Cl^-_{(aq)} + OH^-_{(aq)}$ (2.16)

iv) Oxidation of Hg^0 by ·OH. Lin and Pehkonen (1997) investigated the kinetics of aqueous elemental mercury oxidation by a hydroxyl radical (·OH), employing the steady-state kinetic technique developed by Zepp et al. (1987). The aqueous phase ·OH was produced by nitrate photolysis and benzene was used as the hydroxyl radical scavenger, through this method one can obtain a 3.7 x 10^{-15} M steady-state concentration of the hydroxyl radical. The obtained second order rate constant (Equation 2.17) is 2.0 x 10^9 M^{-1} s^{-1}.

Meanwhile, the authors suggested the following mechanism.

$Hg^{0}_{(aq)} + \cdot OH \rightarrow Hg^{+}_{(aq)} + OH^{-}_{(aq)}$; (2.17)

$Hg^{+}_{(aq)} + \cdot OH \rightarrow Hg^{2+}_{(aq)} + OH^{-}_{(aq)}$ (2.18)

On the other hand, Buxton at al. (1988) reported the rate constant of Equation 2.18 to be ~ 10^{10} M^{-1} s^{-1}. However, this is essentially a diffusion-limited rate constant, so the rate of Hg^{0}-oxidation by ·OH is controlled by Equation 2.17.

2.1.2 REDUCTION PATHWAYS

To date, the identified pathways of divalent mercury reduction in the aqueous phase of the atmosphere are divalent mercury reduction by sulfite (SO_3^{2-}) (Munthe et al., 1991), the reduction of Hg^{2+} by hydroperoxyl radicals ($HO_2\cdot$) produced by the photolysis of organic acids (Pehkonen and Lin, 1998), and the photoreduction of mercuric hydroxide (Xiao et al., 1994) .

i)Reduction by Sulfite. Munthe et al. (1991) investigated the divalent mercury reduction by sulfite in aqueous solutions. The proposed mechanism involves the formation of an unstable intermediate, $HgSO_3$, which decomposes rapidly to produce Hg^{+}, which in turn is rapidly reduced to Hg^{0}. The overall rate of the reaction is inversely dependent on the concentration of sulfite with the value of 0.6 s^{-1}.

The mechanism of this reaction suggested by the authors is as follows.

$Hg^{2+} + SO_3^{2-} \rightarrow HgSO_3$ (2.19)

$HgSO_3 + SO_3^{2-} \rightarrow Hg(SO_3)_2^{2-}$ (2.20)

$HgSO_3 \rightarrow Hg^{+} + SO_3^{-}$ (2.21)

$Hg^{+} + HSO_3^{-} \rightarrow Hg^{0} + SO_3^{-} + H^{+}$ (2.22)

Or $Hg^{+} + Hg^{+} \rightarrow Hg^{0} + Hg^{2+}$ (2.23)

The aqueous phase mercury reduction by sulfite is a species-specific process. Divalent mercury and sulfite form two different $HgSO_3$ complexes, which exhibit quite distinct reactivity. $HgSO_3$ is highly unstable and easily decomposes to Hg^+, eventually reducing to Hg^0; while $Hg(SO_3)_2^{2-}$ is a stable complex and does not yield Hg^0 (Munthe et al., 1991). Therefore, it is very important when estimating the reaction rate of Hg^{2+} reduction by sulfite that the mercury sulfite complex speciation distribution is considered.

ii) Reduction by Hydroperoxyl Radical ($HO_2\cdot$). Pehkonen and Lin (1998) studied the aqueous phase reduction of divalent mercury by a hydroperoxyl radical, which is produced by the photolysis of oxalate ($C_2O_4^{2-}$). The proposed chemical scheme involves a production of Hg^+ as the first step and a further reduction of Hg^+ to form Hg^0. Owing to the instability of Hg^+ in the aqueous phase, the authors assumed Eq. (2.24) to be the rate-determining step with a rate constant of $1.7 \times 10^4\ M^{-1}s^{-1}$.

The reaction mechanism of this reaction is as follows.

$$HO_2\cdot + Hg^{2+} \rightarrow Hg^+ + O_2 + H^+ \qquad (2.24)$$

$$HO_2\cdot + Hg^+ \rightarrow Hg^0 + O_2 + H^+ \qquad (2.25)$$

iii) Photoreduction of Mercuric Hydroxide. Xiao et al. (1994) studied the photochemical behavior of $Hg(OH)_2$ and HgS_2^{2-} in water upon irradiation at wavelengths greater than 290 nm. They found that $Hg(OH)_2$ can be photolyzed to produce Hg^0 four times faster than HgS_2^{2-}. While Nriagu (1994) suggested the following mechanism of $Hg(OH)_2$ photoreduction :

$$Hg(OH)_{2(aq)} \xrightarrow{h\nu} [Hg(OH)^*] \rightarrow Hg(OH)_{(aq)} + \cdot OH_{(aq)} \qquad (2.26)$$

$Hg(OH)^*$ shows a complex in an exited state, which is quickly reduced to Hg^0, due to the instability of this complex in atmospheric water.

Xiao et al. (1994) estimated the rate constant of this photoreduction with a value of $3 \times 10^{-7} s^{-1}$.

2.2 CHEMICAL TRANSFORMATIONS IN THE GASEOUS PHASE

Compare to reactions in the aqueous phase, the kinetic data in the gaseous phase are very limited, because many gaseous reactions of mercury with atmospherically important oxidants and/or reductants are difficult to investigate experimentally due to the low concentrations of species in the atmosphere, low volatility of products, and strong effects of heterogeneous reactions which can take place on the wall of a reactor. So far, numerous studies have been published on gaseous mercury reduction and/or oxidation by species in the atmosphere, including gaseous elemental mercury oxidation by ozone, oxidation by methyl radicals, oxidation by hydrogen peroxide, and oxidation by atomic and molecular halogens (chlorine and bromine) (McKeown et al, 1983; Niki, 1983; Lund-thompson and Egsgaard, 1986; Meylan and Howard, 1993; Hall, 1995; Sommar et al., 1996; Tokos et al., 1998). The following discussion focuses on the reactions associated with halogens.

The gaseous phase oxidations of elemental mercury by molecular and atomic chlorine and/or bromine in the atmosphere were investigated by Ariya et al. (2002) using absolute and relative techniques, respectively. They found that the reaction between elemental mercury and molecular chlorine is strongly catalyzed by surfaces. It has been noted that the reaction rate appeared to become accelerated at higher conversions (consuming) of mercury, leading to two kinetic regimes, one is gas-phase reaction with the rate constant of $2.62 \pm 0.08 \times 10^{-18}$ $(cm^3/molecule)$ s^{-1}, the other is surface-

catalyzed reaction, with the rate constant of $4.63 \pm 0.28 \times 10^{-18}$ (cm^3/molecule) s^{-1}, which is believed to be occur after the reaction wall is covered by a product (identified to be $HgCl_2$). However, for the reaction with molecular bromine although there was a failure to observe the two reaction rate regimes, it was found that the reaction is significantly faster than molecular chlorine with the rate constant of $0.9 \pm 0.2 \times 10^{-16}$ (cm^3/molecule) s^{-1}.

In the above experiments, elemental mercury was oxidized by atomic chlorine and/or bromine, and the organic substrates were used as a reference in the kinetic experiments. Because the reactions of mercury and atomic halogens proceed rapidly, the adsorption biasing the kinetics and surface catalysis have not been observed (Ariya et al., 2002). The reported rate constants for the atomic chlorine and bromine are $1.0 \pm 0.2 \times 10^{-11}$ (cm^3/molecule) s^{-1} and $3.2 \pm 0.3 \times 10^{-12}$ (cm^3/molecule) s^{-1}, respectively. The major product of the reaction was identified as $HgCl_2$. Comparing these obtained data, the reactions of Hg^0 with molecular halogens are too slow to be important in atmospheric mercury transformation. Indeed, the reactivities of atomic halogens are the highest; the inferred concentrations of atomic chlorine and bromine and the kinetic data provide evidence that atomic bromine is the only likely responsible species for rapid depletion of mercury in the Arctic (Ariya et al., 2002).

2.3 REDOX REACTION BETWEEN MERCURY AND IRON IONS.

i) Hg^{2+} and/or Hg_2^{2+} and Fe^{2+}. The early studies on the kinetics of the reaction between Hg^{2+} and Fe^{2+} in perchloric acid discovered the slowness of the reaction due to the diamagnetism of Hg^{2+}, the high paramagnetism of Fe^{2+} and the electrostatic repulsion between the two cations (Adamson, 1952; 1960). But the half-lives of the same reaction reported in both studies were inconsistent; i. e. the former data is some three

orders of magnitude shorter than that calculated from the second-order rate constants given in the latter report. Recently, Raposo et al. (2000) reinvestigated this reaction between Hg^{2+} and/or Hg_2^{2+} and Fe^{2+} and discovered that the kinetics was entirely unusual:

The reaction of Hg^{2+} and Fe^{2+} in 1 M perchloric acid solution was found to proceed extremely slowly with a long start-up of initiation phase, followed by a rapid autocatalytic increase in rate. Concurrent with this increase, a yellow-green by-product formed and disappeared again when the reaction came to an end. The by-product was a special form of colloidal mercury with Fe^{2+} attached as a colloid stabilizer. The colloid formation was demonstrated by the Tyndall effect and electrophoresis experiments.

In the related reaction between Hg_2^{2+} and Fe^{2+}, the autocatalytic cycle started near the beginning of the experiment, and the yellow-green by-product again appeared. The proposed mechanism of the reaction between divalent mercury and ferrous iron is as follows:

$Hg^{2+} + Fe^{2+} \rightleftarrows Hg^{+} + Fe^{3+}$	$k_1 = 1.42 \times 10^{-7}\ M^{-1}s^{-1}$ $k_{-1} = 1 \times 10^{-10}\ M^{-1}s^{-1}$	(2.27)
$Hg^{+} + Fe^{2+} \rightleftarrows Hg_c^{0} + Fe^{3+}$	$k_2 = 1.67 \times 10^{-4}\ M^{-1}s^{-1}$ $k_{-2} = 1 \times 10^{-6}\ M^{-1}s^{-1}$	(2.28)
$Hg^{2+} + Hg_c^{0} \rightleftarrows 2Hg^{+}$	$k_3 = 6.67 \times 10^{-5}\ M^{-1}s^{-1}$ $k_{-3} = 1 \times 10^{-6}\ M^{-1}s^{-1}$	(2.29)
$Hg_c^{0} + nFe^{2+} \rightleftarrows [Hg_c^{0} - (Fe^{2+})_n]$	$k_4 = 1.67 \times 10^{-5}\ M^{-1}s^{-1}$ $k_{-41} = 3.3 \times 10^{-6}\ M^{-1}s^{-1}$ $k_{-42} = 1.67 \times 10^{-3}\ M^{-1}s^{-1}$	(2.30)
$2Hg^{+} \rightleftarrows Hg_2^{2+}$	$k_5 = 1.67 \times 10^{-4}\ M^{-1}s^{-1}$ $k_{-5} = 1.67 \times 10^{-9}\ M^{-1}s^{-1}$	(2.31)

The above rate constants are calculated by the computer program called Mercury which is a numerical calculation based on the experimental kinetics by adjusting the parameters to repeat the features of the mechanism. (Raposo et al., 2000).

ii) $Hg^0 + Fe^{3+}$. In 1842, Schaffhäult first recognized the fact that mercury reduces an aqueous solution of ferric chloride. The reaction proceeds more rapidly in the presence of hydrochloric acid. Later, Carnegie (1888) and Borar (1911) observed the same phenomenon and found the reaction can proceed to completion (McCay and Anderson, 1921).

McCay and Anderson (1921) reinvestigated the reaction between elemental mercury by letting the mercury droplets react with aqueous ferric iron and proved again that the reaction proceeded rapidly and completely when shaken in the presence of mercury droplets under the conditions of free acid or no free acid.

The reaction mechanism is as follows:

$2Hg^0 + 2Fe^{3+}$? $2Fe^{2+} + 2Hg^+$ (McCay and Anderson, 1921). (2.32)

iii) $Hg^{2+} + Fe^{3+}$ + OACC (organic acid coordination compound) $\xrightarrow{h\nu}$ DGM (dissolved gaseous mercury). Zhang and Lindberg (2001) irradiated lake water and/or pool water with or without spiking a freshly prepared ferric iron salt and found repeatable and significantly large increases in DGM production. Usually, the reduction with the spiking ferric iron proceeds much faster than that without the ferric iron spike. At the same time, the decrease in DGM was also observed when both water samples were kept in the dark. Such a behavior implicates a redox cycling of Hg characterized by reduction in sunlight and oxidation in the dark, probably occurring simultaneously and both originating photochemically.

(a) Reduction of Hg^{2+} in sunlight. Sunlight-induced photochemical production of highly reducing organic free radicals occurs via the photolysis of Fe^{3+}-organic acid coordination compounds [Fe^{3+}-OACC] and a subsequent reduction of Hg^{2+} by organic free radicals (Zhang and Lindberg, 1999). The sunlight induced photochemical production follows a first-order kinetic scheme, with the rate constant of 0.2 h^{-1} for the lake water and 0.1 h^{-1} for the pond water (Zhang and Lindberg, 2001).

The hypothetical mechanism for such a behavior is as follows:

Fe^{3+} + natural organic acids ? Fe^{3+}-OACC (2.33)

Fe^{3+}-OACC + $h\nu$? Fe^{2+} + organic free radicals (2.34)

Organic free radicals + Hg^{2+} ? Hg^{0} + products + CO_2 (2.35)

(b) Oxidation in the dark. Dark oxidation of Hg^{0} by photochemically originated oxidants has been also observed (Cooper et al., 1994; Zou and Hoigne, 1992; Zhang and Lindberg, 1999). The DGM decrease in the dark exhibited an apparent first-order kinetics, with the rate constant of 0.2 h^{-1} with the Fe^{3+} spike and 0.3 h^{-1} without the Fe^{3+} spike.

The hypothetical mechanism in the dark is as follows:

Organic free radicals + O_2 ? $\cdot O_2^-$ + products + CO_2 (2.36)

DOC + $h\nu$? DOC* (2.37)

DOC* + O_2 ? $\cdot DOC^+$ + $\cdot O_2^-$ (2.38)

$\cdot O_2^-$ + $\cdot O_2^-$ + $2H^+$? H_2O_2 + O_2 (2.39)

H_2O_2 + Fe^{2+} ? $\cdot OH$ + OH^- + Fe^{3+} (2.40)

$2\cdot OH$ + Hg^{0} ? Hg^{2+} + $2OH^-$ (2.41)

Another possible reduction of Hg^{2+} might be related to dissolved oxygen (DO) (Pehkonen and Lin, 1998):

$\cdot O_2^-$ + Hg^{2+} ? Hg^{0} + O_2 (2.42)

Moreover, ·OH might also be produced in natural water via direct photolysis of DOC (Vaughan and Blough, 1998):

$$DOC + H_2O + h\nu \;?\; \cdot OH + \text{products} \qquad (2.43)$$

iv) $Hg^0 \xrightarrow{h\nu} Hg^{2+}$. Lalonde et al. (2001) investigated the photooxidation of $Hg^0_{(aq)}$ in aquatic systems irritated by a UV-B light source. The authors found a significant decrease in Hg^0 in artificial solutions containing both chloride ions and benzoquinone by irradiating with a UV-B light source. On the other hand, more significant photooxidation also occurred in natural waters spiked with $Hg^0_{(aq)}$. The photooxidation of Hg^0 follows pseudo-first-order kinetics with a rate constant of 0.6 h^{-1}. Therefore, such a discovery indicates that the dominant Hg^0 sink is likely to be photooxidation rather than volatilization from the water column during summer days. Nevertheless, Amyot et al. (2000) observed an initial first-order rate constant for Hg^{2+} photoreduction in freshwater to be between 1 and 2 h^{-1}. After normalizing the photon fluxes used in the two experiments, it is found that the light induced redox processes, Hg^{2+} reduction and Hg^0 oxidation, could occur at roughly similar rates in natural water systems, provided that the reaction rates observed in water samples incubated under a UV-B lamp would be equivalent to those incubated under sunlight (Laldone et al., 2001).

CHAPTER 3

OBJECTIVES AND SCOPE

At present, it is widely accepted that Hg^0 vapor constitutes by far the largest component of the total gaseous mercury concentration in the troposphere. Hg^0 should play a pivotal role in the atmospheric chemistry of this heavy metal. Although numerous investigators have contributed to the understanding of this toxic metal recycling in the atmosphere, as described in the previous section, the knowledge in this area is still far from complete. To better understand the global cycle of this toxic metal in the environment and the contribution to the polar spring mercury increases, the kinetics and mechanisms of reactions of aqueous elemental mercury oxidized by aqueous bromine species (bromine, hypobromous acid and hypobromite) need to be studied. Therefore, this study discusses the kinetics of elemental aqueous mercury oxidation by bromine, hypobromous acid and hypobromite. A comparison between atmospherically important oxidants is carried out to determine whether the aqueous bromine species play a significant role in the oxidation of mercury in the atmosphere.

On the other hand, since numerous researchers have focused on mercury and iron from the last century, significant findings about mercury and iron have been discovered (McCay and Anderson, 1921; Adamson, 1952; 1960; Amyot et al. 2000; Raposo et al., 2000; Laldone et al., 2001; Zhang and Lindberg, 2001). The early information about the reaction rate of element and ferric iron was obtained by allowing elemental mercury droplets to react with a ferric iron solution. However, it is not known whether these results obtained with liquid drops of Hg^0 are relevant to natural waters containing low concentrations of dissolved elemental mercury, $Hg^0_{(aq)}$. Furthermore, the quantitative rate constants of natural iron-mercury redox cycling are still uncertain. Moreover, many findings have suggested an interesting redox behavior between mercury and iron, but the knowledge on the relationship between Fe and aquatic Hg photochemodynamics is still limited. The objective of this study is to investigate the

following redox reaction involving iron and mercury and focus on the aforementioned areas.

$Hg^{2+} + 2Fe^{2+} \rightleftharpoons Hg^{0} + 2Fe^{3+}$ (McCay and Anderson, 1921) (3.1)

CHAPTER 4

EXPERIMENTAL AND REACTION SETUP

4.1 REAGENTS

Material. Elemental mercury (99.9995%), mercuric chloride (99.5%), bromine (99.5%), ferric sulphate (97%), ferrous sulphate (99%), sodium perchlorate, perchloric acid (70%), sodium sulfite, sodium dihydrogen phosphate, sodium phosphate monobasic monohydrate and sodium hydroxide, Ferrozine, hydrochloric acid, ammonium acetate, ammonium hydroxide, sodium fluoride, sulfuric acid (95~98%), chloroform (99.4%) and dithizone are all of reagent grade and were used as received.

Elemental mercury solution. Solutions of elemental mercury were prepared by stirring 0.5 ml of liquid mercury droplet in a 1L Teflon (FEP) bottle with oxygen-free ultrapure (Millipore®) water for eleven or thirteen hours without leaving any head space in the FEP bottle to eliminate the evaporation of mercury and its oxidation by dissolved oxygen. Before stirring, the liquid mercury was washed two times by 0.1 M perchloric acid and two times by deionized water to remove the oxidized Hg compounds from its surface. The concentrations of elemental mercury solution obtained in this way, usually around 0.8 ~ 2.1 x 10^{-7} M, were somewhat below the reported solubility limit of metallic mercury in water, 3.03 x 10^{-7} M at 298 K (Clever et at., 1985), which was probably due to small losses during the transfer of the solution to the reaction vessel.

Stock sulfite Solution. A stock sulfite solution was prepared from sodium sulfite solid, which was dissolved in ultrapure (Millipore®) water. Fresh aqueous sulfite solutions were prepared before each experiment, owing to the relatively rapid auto-oxidation of sulfite in aqueous solution containing dissolved oxygen.

Bromine

i) Physical and Chemical Properties of Bromine. Bromine is a brown-red, fuming, heavy and highly corrosive liquid with a specific gravity of nearly 3.12 at 20^0C. It is the only non-metallic element liquid at room temperature; it freezes at -7.3^0C and boils at 58.8^0C. The atomic number of bromine is 35. The outermost arrangement of the electrons is $4s^2 4p^5$. The common valence of bromine is -1.

ii) Reactivity. Many reactions of bromine are related to its oxidizing power as expressed by the equation below:

$$Br^- \rightleftharpoons 1/2\ Br_2 + e^- \qquad (4.1)$$

The standard potential, E^0, for this reaction is -1.065 volts (Latimer, 1939). Bromine has the ability to oxidize a large number of species that are less electronegative in character. Much of the chemistry of bromine is associated to its reaction with water. At 25^0C, bromine dissolves in water to the extent of 33.6 g/l (0.21 mol/L). $Br_{(aq)}$ reacts with water, through a disproportionation reaction, with one atom being oxidized to Br(+1), the other being reduced to Br(-1).

The following equilibrium exists in solution:

$$Br_2 + H_2O \rightleftharpoons H^+ + Br^- + HOBr \qquad \log K = 8.24 \qquad (4.2)$$

The slight ionization of hypobromous acid:

$$HOBr \rightleftharpoons H^+ + BrO^- \qquad \log K = 8.60 \qquad (4.3)$$

Hypobromous acid is rather unstable and exists only in dilute solutions with a saturation concentration of about 67 percent with a faint yellow color and odor of jasmine. It is a weak acid having a dissociation constant of about 2×10^{-9}. It is a good oxidizing agent. When exposed to light it decomposes with the evolution of oxygen:

$$2HBrO \rightleftharpoons 2HBr + O_2 \qquad (4.4)$$

$$HBrO + HBr \rightleftharpoons Br_2 + H_2O \qquad (4.5)$$

When in strong alkali solutions, bromine is converted to hypobromite, which is relatively stable at low temperatures. It will generate bromide ions in an amount equal to 50 percent of the total bromine present.

$Br_2 + 2NaOH \rightarrow NaOBr + NaBr + H_2O$ (4.6)

iii) The composition of bromine solutions. The composition of bromine solutions is governed by the following three equations (drived by Lewin, 1966):

$[H^+]\,[BrO^-] = K_d\,[HBr]$ $\qquad K_d = 2 \times 10^{-9}$ (4.7)

$[H^+]\,[Br^-]\,[HBrO] = K_h\,[Br_2]$ $\qquad K_h = 5.8 \times 10^{-9}$ (4.8)

$[Br^-][Br_2] = K_c[Br_3^-]$ $\qquad K_c = 0.063$ (4.9)

The bromine solutions are therefore composed of four oxidizing agents:

$C_{T,Br} = [Br_2] + [HBrO] + [BrO^-] + [Br_3^-]$ (4.10)

The concentrations of the components can be determined by solving the above equations, assuming constant $[Br^-]$, as follows (derived by Lewin, 1966),

$$a_{[Br^2]} = (1 + \frac{K_h}{[H^+][Br^-]} + \frac{K_d K_h}{[H^+]^2[Br^-]} + \frac{[Br^-]}{K_c})^{-1} \quad (4.11)$$

$$a_{[HOBr]} = (1 + \frac{[H^+][Br^-]}{K_h} + \frac{K_d}{[H^+]} + \frac{[Br^-]^2[H^+]}{K_c K_h})^{-1} \quad (4.12)$$

$$a_{[OBr^-]} = (1 + \frac{[H^+]}{K_d} + \frac{[H^+]^2[Br^-]}{K_h K_d} + \frac{[Br^-]^2[H^+]^2}{K_h K_d K_c})^{-1} \quad (4.13)$$

$$a_{[Br_3-]} = (1 + \frac{Kc}{[Br^-]} + \frac{K_c K_h}{[H^+]\,[Br^-]^2} + \frac{K_c K_d K_h}{[H^+]^2[Br^-]^2})^{-1} \quad (4.14)$$

Using these equations, the composition of the solutions over the entire pH range of 0~14 and a wide range of bromine concentrations can be easily calculated.

Figures 4.1 and 4.2 show the bromine speciation distribution as a function of pH at different bromine concentrations. It can be clearly observed from the figures that below pH of 3, bromine is present almost entirely as aqueous molecular Br_2. Above

pH of 3, the fraction present as Br_2 decreases and HOBr is formed. Between pH of 6 and 8, where most of the bromine is present as HOBr, little change in activity is found. Between pH 8 and 10, HOBr decreases, whereas hypobromite, OBr^-, increases rapidly and becomes the predominant species.

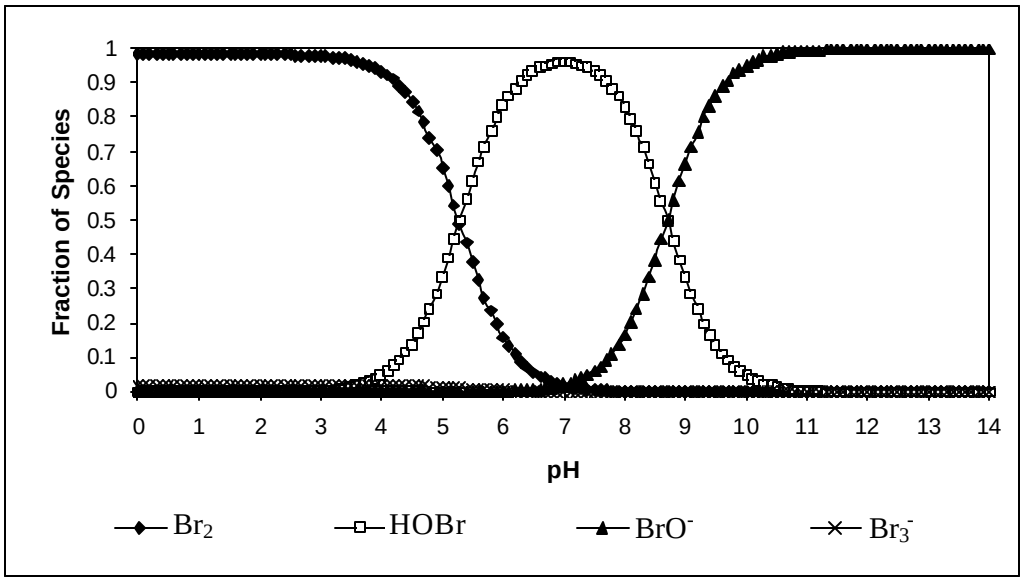

Figure 4.1 Speciation of bromine as a function of pH. Concentration: [Br_{tot}] =1.125 mM.

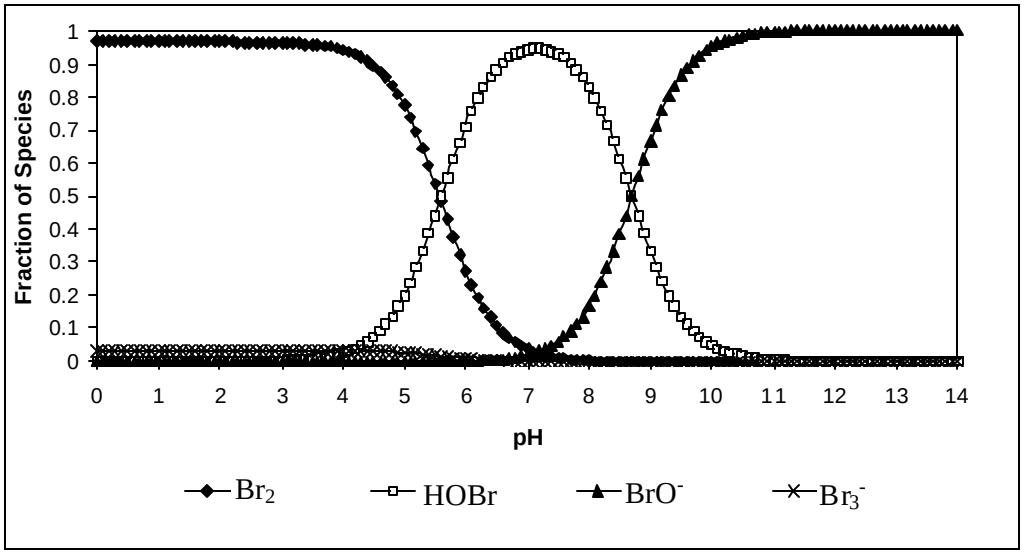

Figure 4.2 Speciation of bromine as a function of pH. Concentration: [Br_{tot}] =2.25 mM.

4.2 REACTION SETUP

4.2.1 REACTIONS BETWEEN ELEMENTAL MERCURY AND BROMINE SPECIES

The kinetic study was conducted by letting dissolved Hg^0 react with excess bromine species at concentrations of 1.125 and 2.25 mM at pH values of 2, 6.8 and ~ 12 in a 500-ml Teflon reactor at room temperature (20~23°C) in the dark with continuous stirring. The vessel was sealed and covered with aluminum foil to isolate the solution from the atmosphere in order to eliminate the evaporation of elemental mercury and the possible interference by dissolved oxygen and the interference of light. Experiments were carried out under the nitrogen environment at all the time, to eliminate the additional oxidation by oxygen. Aerosols are usually highly concentrated solutions. Laboratory measurements show that NaCl molalities in droplets can be in excess of 10 mol/kg (Tang, 1997) indicating a very high ionic strength. For all the experiments, 0.1 M sodium perchlorate was used to keep a constant ionic strength. The kinetics of the oxidation of elemental mercury was investigated by measuring the change in a certain UV absorption band, which is the maximum absorption of the mercury-dithizone complex. Absorbance and time were recorded. For each selected pH value of 2.9 6.8 and 12, the dominant species is bromine, hypobromous acid and hypobromite, respectively.

4.2.1.1 Mercury determination

Divalent mercury concentrations were measured by a modified dithizone method (Eaton et al., 1986). After extraction of the aqueous mercury aliquot into chloroform containing ~ 1.38×10^{-4} M or 2.76×10^{-4} M of dithizone, absorbance measurements of the chloroform phase were obtained at 496nm by a Shimadzu UV-1601 UV-VIS

spectrophotometer. Using a 1-cm cuvette and a volume ratio of aqueous to organic of 10 to 1, the detection limit is ~ 1.0 x 10^{-8} M. Total elemental mercury was measured as Hg^{2+} after oxidation it to the divalent state by potassium permanganate, as described in Standard Methods (Eaton et al., 1986). We assume that all the elemental mercury was oxidized to divalent mercury, since the monovalent mercury is not stable and not very likely in the system (McElroy and Munthe, 1991; Martell et al., 1993; Lin and Pehkonen, 1997).

Usually the aqueous solution containing mercury was acidified before extraction with chloroform-dithizone to eliminate the interference of other heavy metals and to avoid the color degradation of dithizonate upon exposure to strong light. However, for the system containing halides, at high acidities excess halides hinder the extraction of mercury (see Results and Discussion). Sandell (1959) have suggested that for the solution containing iodide or bromine, which are complex-forming agents with mercury, at pH of 6, the mercury can be practically all extracted from a 0.05M potassium iodide solution. However, when a solution of dithizone in an organic solvent is shaken with an alkaline aqueous solution, excess dithizone will be transferred virtually completely to the aqueous phase and dithizone dissolves with a yellow color to give the alkali metal dithizonate, which may be considered to be completely dissociated. Such a change of color from greenish to yellow interferes with the mercury determination by the dithizone method. Based on these points, a neutral aqueous solution and concentrated chloroform-dithizone solution (up to 2.76 x 10^{-4} M) were used to achieve accuracy of this analysis.

4.2.2 REACTION BETWEEN MERCURY AND IRON IONS

4.2.2.1 The backward reaction of Fe^{3+} and Hg^{0}

The kinetic study was conducted by letting dissolved Hg^0 react with excess free ferric iron at pH of ~ 2.9 in a 500 ml Teflon bottle at room temperature (23~25°C) in the dark. The vessel was sealed to isolate the solution from the atmosphere in order to eliminate the evaporation of elemental mercury and the possible interference by dissolved oxygen. Experiments were carried out under the nitrogen environment at all times, to eliminate the additional oxidation by oxygen. The reaction medium was maintained at pH of ~ 2.9 with perchloric acid in all experiments. Higher pH values were not attempted due to experimental complications, such as ferrous iron oxidation by dissolved oxygen, ferric iron hydroxide precipitation, and also reactant and product ion hydrolyses.

4.2.2.2 The forward reaction between Hg^{2+} and Fe^{2+}

A 250 ml Teflon reactor vessel, containing 150 ml of aqueous solution, was stirred with a magnetic stirrer during the course of the experiment to achieve a homogeneous solution. The irradiation beam was directed to the top opening of the vessel without passing through the Teflon wall. The wavelengths of irradiation from a 450 W Xenon Universal Arc Lamp Housing, of wavelengths above 285 nm and intensity 1.50 mW/cm^2 at 312 nm (Oriel Corp. Model 66921) were controlled by the use of filters (Oriel Corp. Model 59423 and 59450) with appropriate windows of transmission. Two neutral density filters with different nominal absorbances were used to decrease the light intensity in the experiments. The irradiation experiments were carried out at three pH values: 2.2, 2.5, 2.9. The pH range was selected in a way that higher pH values were omitted to prevent ferrous iron oxidation by dissolved oxygen, ferric hydroxide precipitation, and also reactant and product ion hydrolyses. The pH change during the experiment was limited to 0.1 pH units. The irradiation experiments were carried out

with a fixed initial divalent mercury concentration of 3 µM and a ferrous ion concentration of 5 and 8 µM. Dark control experiments were also carried out to eliminate the possibility of adsorption of mercury to the walls of the reactor to account for the observed concentration profiles.

Two bandpass filters (Model 59423 and 59450) and two neutral density filters (Model 59660 and 59680) were used individually. For long pass filters, model 59420 cuts off wavelengths less than 285 nm, while model 59450 cuts off wavelengths less than 309 nm (a window of transmission from 285 to 800 nm or from 309 to 800 nm). For neutral density filters, model 59660 has a nominal absorbance of 0.2 (~60% transmittance), while model 59680 has a nominal absorbance of 0.4 (~40% transmittance).

4.2.2.3 Mercury determination

Divalent mercury was measured by a modified dithizone method (Eaton et al., 1986), after extraction of the aqueous aliquot into chloroform containing ~ 1.3 x 10^{-5} M dithizone. Absorbance measurements of the chloroform phase were obtained at 496 nm by a Shimadzu UV-1601 UV-VIS spectrophotometer. With a 1-cm cuvette and a volume ratio of 10 to 1, the detection limit is ~ 1.0 x 10^{-8} M. Elemental mercury was measured as Hg^{2+} after oxidation to the divalent state by potassium permanganate as described in Standard Methods (Eaton et al., 1986).

4.2.2.4 Ferrous iron determination

Ferrous iron concentrations were measured by a Ferrozine method (Stookey, 1970). The presence of ferric iron, Fe^{3+}, can interfere with the Ferrozine method (Viollier et al., 2000), thereby affecting the accuracy of the method. Thus, ~0.03 M NaF was

added to the extraction solution before the measurement. Fluoride, being a strong ligand for Fe^{3+}, will mask the ferric iron for ferrous ion determination to succeed. The detection limit is ~ 1.25×10^{-7} M.

CHAPTER 5

RESULTS AND DISCUSSION

5.1 REACTIONS BETWEEN ELEMENTAL MERCURY AND BROMINE SPECIES

5.1.1 THE EFFECT OF COMPLEXING AGENT AND pH SELECTION IN THE MERCURY DETERMINATION

When using the ditionzone method to determine mercury concentrations, the complex forming agent with mercury, the excess alkali and even weak oxidant will affect the accuracy of this method. Such interferences can be eliminated in the neutral solution, and enhance the accuracy of the measurement.

5.1.1.1 Distribution of dithizone between aqueous phase and organic phase for the case, in which containing an ion X^- complexes Hg^{2+}.

Dithizone is a dibasic acid, and its dissociation has the following equilibria,

H_2D_z ? $H^+ + HD_z^-$, (5.1)

HD_z^- $H^+ + D_z^-$. (5.2)

The metal ions which complex with dithizone in an immiscible organic solvent are be assumed as divalent form for simplicity. The reversible reaction between metal ions and dithizone in the organic solvent is expressed as follows.

$Me^{2+} + 2H_2D_z$? $Me(HD_z)_2 + 2H^+$

The equilibrium constant for this reaction is (derived by Sandell 1959),

$$K = \frac{[Me(HD_z)_2]_o[H^+]^2}{[Me^{2+}][H_2Dz]_o^2}.$$

Then the expression for the extraction coefficient of the metal can be arranged as follows (derived by Sandell 1959),

$$E_{Me} = \frac{\sum[Me]_o}{\sum[Me]_w} = \frac{[Me(HD_z)_2]_o}{[Me^{2+}]}$$

To simplify the calculation, assume that the only metal species in the aqueous solution are Me^{2+}, $Me(OH)^+$, $Me(OH)_2$, $Me(OH)_3^-$, and $Me(OH)_4^{2-}$, the general expression for

the extraction coefficient of dithizonate, whether in basic or acidic solutions can be derived as follows (derived by Sandell 1959):

$$\sum [Me]_w = [Me^{2+}] + [Me(OH)^+] + [Me(OH)_2] + [Me(OH)_3^-] + [Me(OH)_4^{2-}]$$

$$= [Me^{2+}] + \frac{K_1[Me^{2+}]}{[H^+]} + \frac{K_2[Me^{2+}]}{[H^+]^2} + \frac{K_3[Me^{2+}]}{[H^+]^3} + \frac{K_4[Me^{2+}]}{[H^+]^4} \tag{5.3}$$

where the K values (i.e. hydrolysis constants) are defined as follows:

$$K_1 = [Me(OH)^+][H^+] / [Me^{2+}] \tag{5.4}$$

$$K_2 = [Me(OH)]_2[H^+]^2 / [Me^{2+}] \tag{5.5}$$

$$K_3 = [Me(OH)_3^-][H^+]^3 / [Me^{2+}] \tag{5.6}$$

$$K_4 = [Me(OH)_4^{2-}][H^+]^4 / [Me^{2+}] \tag{5.7}$$

$$\therefore E_{Me} = \frac{[Me(HD_z)_2]_o}{\sum [Me]_w} = K[H_2D_z]^2_o \times \frac{1}{1 + \frac{K_1}{[H^+]} + \frac{K_2}{[H^+]^2} + \frac{K_3}{[H^+]^3} + \frac{K_4}{[H^+]^4}} \tag{5.8}$$

If the aqueous solution contains an ion X^- complexing Me^{2+}, the expression for the extraction coefficient becomes (derived by Sandell 1959)

$$E'_{Me} = \frac{[Me(HD_z)_2]_o}{\sum [Me]_w}$$

$$= \frac{K[H_2D_z]^2_o}{[H^+]^2 \left\{ 1 + \frac{K_1}{[H^+]} + \frac{K_2}{[H^+]^2} + \frac{K_3}{[H^+]^3} \cdots + K_{x1}[X^-] + K_{x2}[X^-]^2 \right\}} \tag{5.9}$$

where the complexation constants are defined as follows:

$$K_{x1} = \frac{[MeX^+]}{[Me^{2+}][X^-]} \tag{5.10}$$

$$K_{x2} = \frac{[MeX_2]}{[Me^{2+}][X^-]^2}, etc \tag{5.11}$$

To simplify the calculation, there is an assumption that the only metal species in the aqueous solution are Hg^{2+}, $HgOH^{+}$, $Hg(OH)_2$. Table 5.1 shows a comparison of distribution of dithizonate between aqueous and organic phases at fixed pH values. It is shown that bromine, being an agent of complexation for divalent mercury actually affects the dithizonate partioning between the aqueous and the organic phase.

5.1.1.2 pH value selection in the determination of mercury concentration

In general, metals, such as Pd, Au, Hg, Au, and Cu can be extracted from a solution with a chloroform solvent containing dithizone. The reaction between metal ion and dithizone takes place in the aqueous phase. Once formed, the metal dithizonate is rapidly transferred to the organic solvent phase. Thus the distribution of dithizonate between the aqueous solution and the organic solution will strongly affect the accuracy of determination. In the reaction system of bromine species and metallic mercury, mercury complexation by bromide, being a strong complexing ligand with divalent mercury, must be taken into account. Figures 5.1 and 5.2 show the aqueous-phase Hg^{2+} speciation as a function of pH at different bromide concentrations (1.125 mM and 2.25 mM). In this reaction system, for the two concentrations of bromide used in the modeling, the predominant mercury species are $HgBr_2$ and $HgBr_3^-$.

Figures 5.3 and 5.4 show the Hg^{2+} speciation distribution varying with pH after adding sulfite to the reaction system. Sulfite is used to quench the excess bromine. From these figures, after adding the sulfite, the predominant species changes from $HgBr_2$ and $HgBr_3^-$ to $Hg(SO_3)_2^{2-}$. Although it was reported that Hg^{2+} can be reduced by aqueous S(IV) (Munthe et al., 1991), according Figures 5.3 and 5.4, the dominant species is $Hg(SO_3)_2^{2-}$ after the addition of sulfite, which is a stable complex and does not reduce to Hg^0 (Munthe et at., 1991). Moreover, Figure 5.5 shows calculated rates of

Table 5.1 A Comparison of Distribution of Dithizonate between Aqueous and Organic Phases at Different pH Values

species	With the complexing agent Br^-		Without the complexing agent Br^-	
Stability Constant	$Hg^{2+} + Br^- \rightleftharpoons HgBr^+$;	K_1=9.05 (1)	$Hg^{2+} + H_2O \rightleftharpoons Hg(OH)^+ + H^+$;	K_1=-3.1 (2)
	$HgBr^+ + Br^- \rightleftharpoons HgBr_2^0$;	K_2=8.28 (1)	$Hg(OH)^+ + H_2O \rightleftharpoons Hg(OH)_2 + H^+$;	K_2=-2.6 (2)
	$HgBr_2^0 + Br^- \rightleftharpoons HgBr_3^-$;	K_3=2.41 (1)	(2) (Heitanen and Sillé n, 1952)	
	$HgBr_3^- + Br^- \rightleftharpoons HgBr_4^{2-}$;	K_4=1.26 (1)		
	(1) (Bethge et al., 1948)			
Equation	$E'_{Me} = \frac{K[H_2Dz]^2_o}{[H^+]^2\left\{1+\frac{K_1}{[H^+]}+\frac{K_2}{[H^+]^2}+\frac{K_3}{[H^+]^3}\cdots+K_{x1}[X^-]+K_{x2}[X^-]^2\right\}}$		$E_{Me} = \frac{K[H_2Dz]^2_0}{[H^+]^2+K_1[H^+]+K_2+\frac{K_3}{[H^+]}+\frac{K_4}{[H^+]^2}}$	
	Where K is extraction constant of dithizonate.		Where K is extraction constant of dithizonate.	
Result	$4.6 \times 10^{-12} K[H_2D_z]^2_o$		$9568K[H_2D_z]^2_o$	
Conclusion	The bromide definitely affects the partitioning of mercury between the aqueous and the organic phase.			

Remark: Both systems contain the same amount of dithizone and calculated under the same pH conditions.

$Hg(SO_3)_2^{2-}$ reduction in cloud- or rain water at different pH values and gas-phase concentrations of SO_2 (Munthe et al., 1991). It can be concluded from this figure that the rate of conversion of $Hg(SO_3)_2^{2-}$ to Hg^0 becomes insignificant at higher pH values, and the conversion rate changes to almost zero at pH above 6.

Considering the above mentioned reasons, a neutral pH is used in the determination of mercury concentration by the dithizone method to eliminate the effect of mercuric bromide complexes and Hg^{2+} reduction by sulfite.

Figures 5.6 and 5.7 show the calibration curves of mercury determination by the dithizone method conducted at different pH values, namely under neutral or acidic conditions. Experiments that extracted a given divalent mercury from the dithizone-chloroform phase at different pH values show that calibration curves can maintain the same slope for different concentrations of bromide, if the extraction was conducted at neutral pH. Thus supports the neutral pH value is more correct for the mercury determination by the dithizone method.

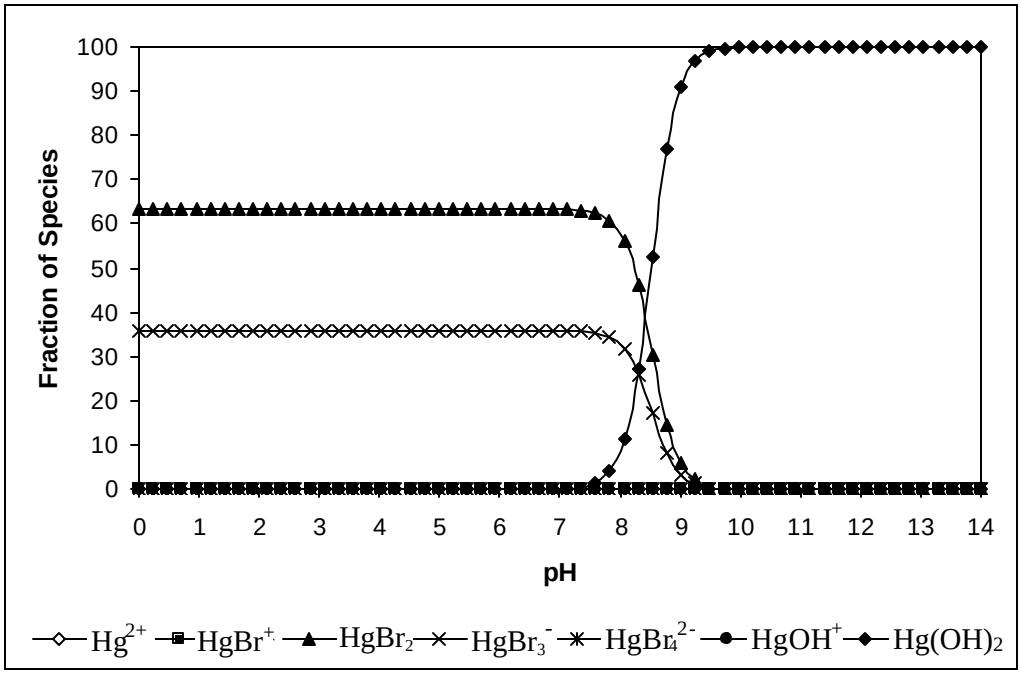

Figure 5.1 Speciation of divalent mercury species as a function of pH.
Concentration: $[Hg^{2+}] = 0.1\ \mu M$, $[Br_{tot}] = 1.125$ mM.

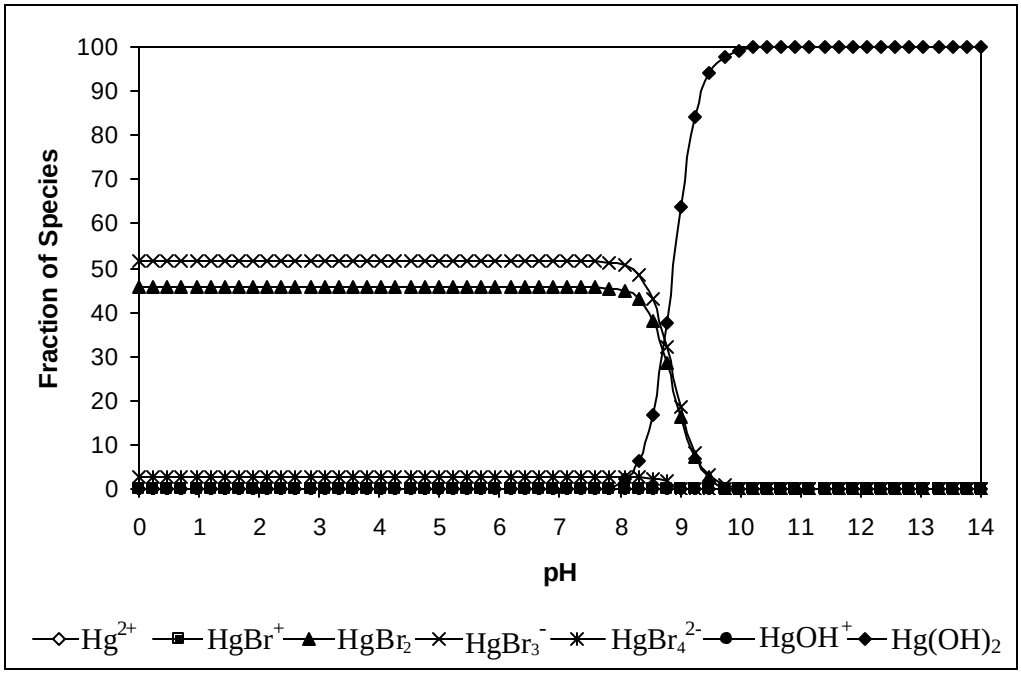

Figure 5.2 Speciation of divalent mercury species as a function of pH.
Concentration: $[Hg^{2+}] = 0.1\ \mu M$, $[Br_{tot}] = 2.25$ mM.

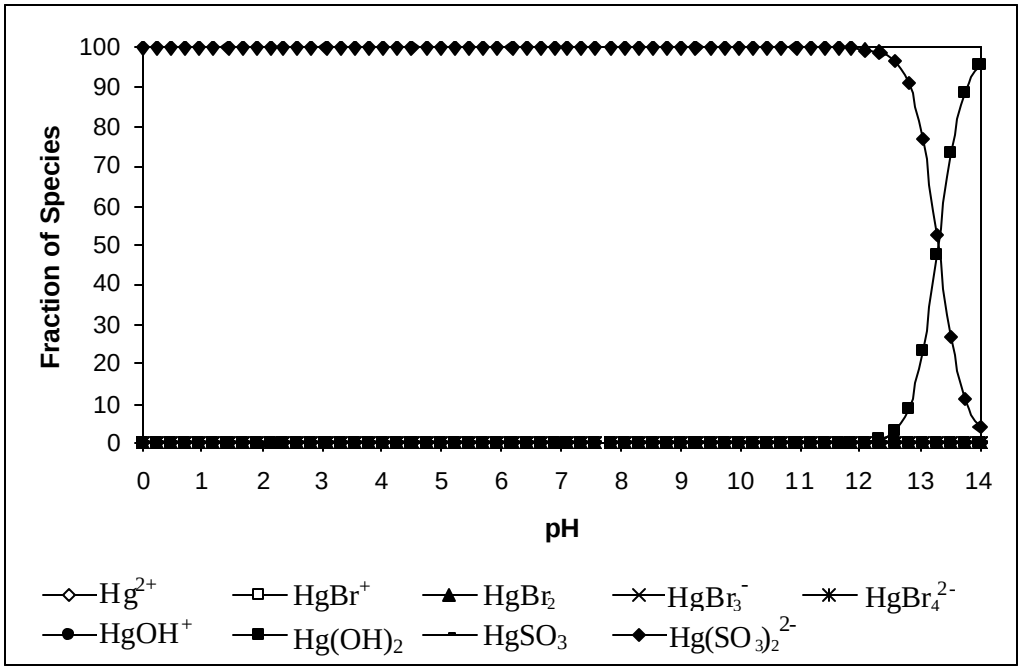

Figure 5.3 Speciation of divalent mercury species as a function of pH after the addition of sulfite to quench the excess bromine.
Concentration: $[Hg^{2+}] = 0.1\ \mu M$, $[Br_{tot}] = 1.125$ mM.

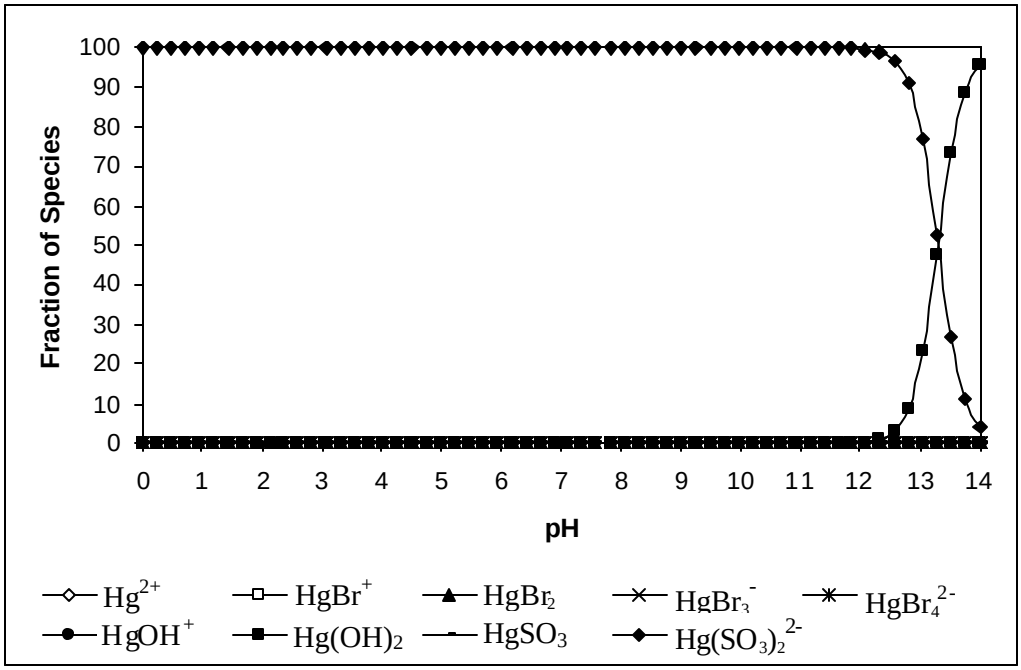

Figure 5.4 Speciation of divalent mercury species as a function of pH after the addition of sulfite to quench the excess bromine.
Concentration: $[Hg^{2+}] = 0.1\ \mu M$, $[Br_{tot}] = 2.25$ mM.

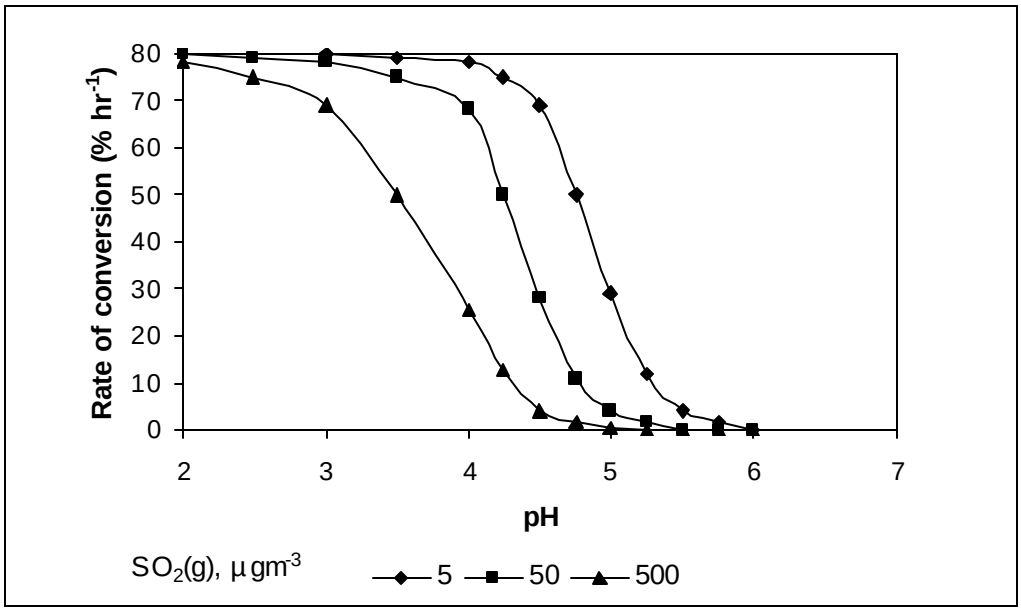

Figure 5.5 Calculated rates of reduction of $Hg(SO_3)_2^{2-}$ in cloud- or rain water at different pH values and gas-phase concentrations of SO_2 (Munthe et al., 1991).

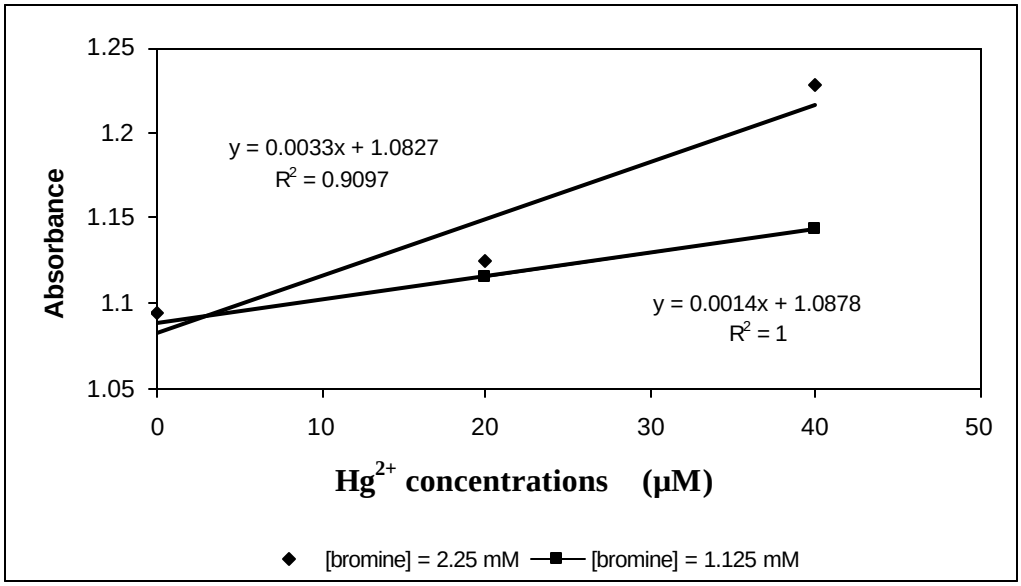

Figure 5.6 Calibration curves of mercury determination by the dithizone method conducted under acidic conditions, e. g., pH of 2.

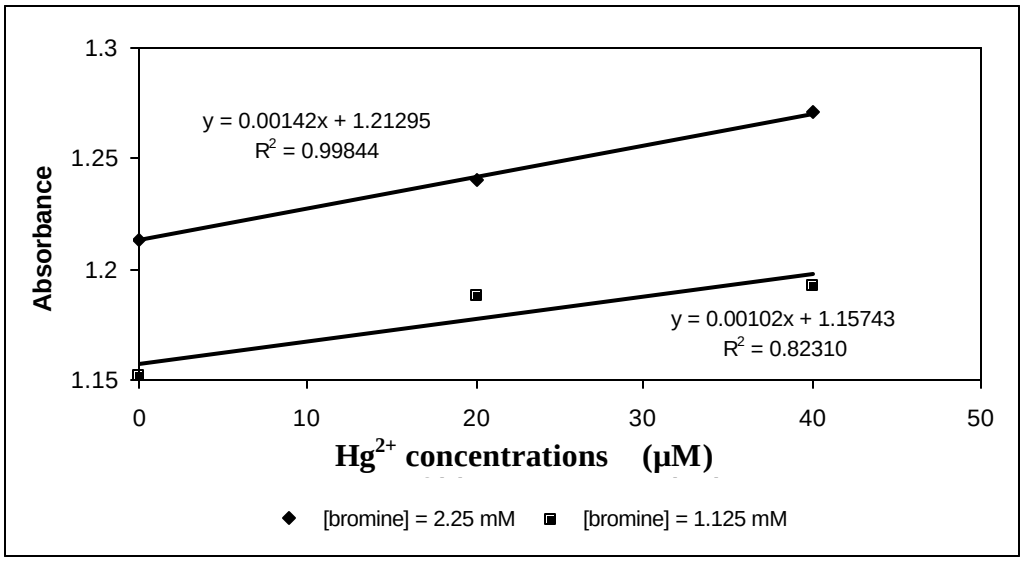

Figure 5.7 Calibration curves of mercury determination by the dithizone method conducted at neutral pH conditions, e. g., pH of 6.8.

5.1.2 KINETICS OF ELEMENTAL MERCURY AND BROMINE SPECIES REACTION

5.1.2.1 Hg^0 and Br_2 at pH of 2

Even under weakly oxidizing conditions, dithizone is oxidizedtodiphenylthiocarbadiazone, which is insoluble in acidic and basic aqueous solutions, but it dissolves in chloroform to give a yellow or brown solution. Moreover, it does not react with metals and as a consequence interferes with the mercury determination by the dithizone method (Sandell, 1959). To eliminate this interference before the mercury determination, 0.066 M freshly prepared sodium sulfite was added to discharge the excess free oxidizing agents, such as bromine, hypobromous acid and hypobromite. It was reported that $HgSO_3$ can be reduced to Hg^0 with rate constant of 0.6 s^{-1}. A concentrated sulfite solution was used in order to form a stable complex of $Hg(SO_3)_2^{2-}$ and a neutral pH value eliminated the reduction of Hg^{2+} by sulfite. However, the reduction of Hg^{2+} by sulfite is a function of pH and the concentration of S(IV). When the sulfite concentration is constant, the reduction rate depends only on pH. Munthe et al. (1991) suggested that no matter what the concentrations of $SO_2(g)$, the rate of conversion of $Hg(SO_3)_2^{2-}$ to Hg^0 is insignificant when the pH value is higher than 6. Divalent mercury and sulfite readily form a $HgSO_3$ complex in the aqueous solution. However, as the concentration of SO_3^{2-} increases, most Hg^{2+} becomes complexed as $Hg(SO_3)_2^{2-}$, which is not as rapidly reduced to Hg^0 as $HgSO_3$, and therefore, the rate of reduction of divalent mercury by sulfite is decreased dramatically. Moreover, it was also reported that no loss of Hg^{2+} was observed when control experiments of Hg^{2+} and S(IV) were performed (Lin and Pehkonen, 1997) .

The first series of experiments were performed to investigate the reaction between Hg^0 and bromine at pH of 2 by using the initial concentrations of elemental mercury of

$0.21\sim0.13 \times 10^{-7}$ M and the concentration of bromine at 1.125 mM and 2.25 mM at room temperature (20~23°C) in the dark. Perchloric acid was used to control the pH value, and pH change during the course of the experiments was limited to ± 0.2 units. The predominant species at this pH is aqueous bromine. The color of the reaction solution is pale yellow.

Figure 5.8 shows the reaction trends of aqueous elemental mercury and aqueous bromine conducted at different bromine concentrations. According to this figure, elemental mercury can be oxidized in the presence of aqueous bromine. The concentration of metallic mercury decreases with time. Figure 5.9 shows that linear profiles were obtained from plots of $\ln(C/C_0)$ vs. time. They indicate the pseudo-first-order behavior typically found in the kinetic experiments. The scopes of the plots were taken as the observed pseudo first-order rate constants.

Table 5.2 shows a compilation of the measured first-order rate constants (k'_{obs}) for the rate of oxidation of elemental mercury in the presence of excess bromine and the derived second-order rate constants (k), which is 0.196 ± 0.03 $M^{-1}s^{-1}$. Furthermore, based on comparison of values of R^2 which derived upon zero and first order kinetic equations, the oxidation of elemental mercury by bromine at pH 2 is more like first order reaction.

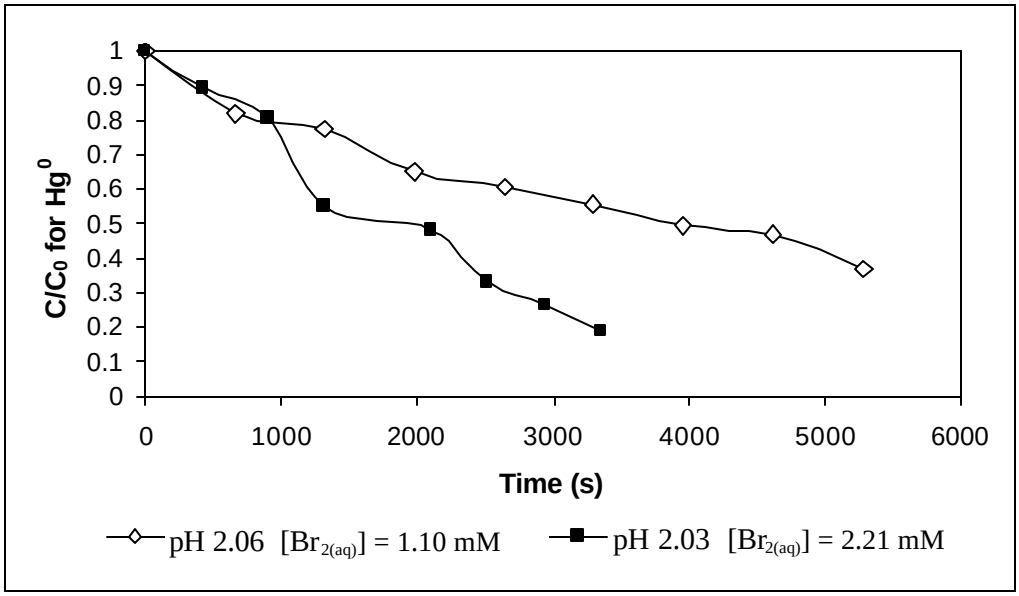

Figure 5.8 Oxidation of aqueous elemental mercury with aqueous bromine (Br_2) at pH 2. Initial reactant concentrations: pH 2.06 [Hg^0] = 0.21 μ M, [Br_2] =1.10 mM;
pH 2.03 [Hg^0] = 0.13 μ M, [Br_2] = 2.21 mM.

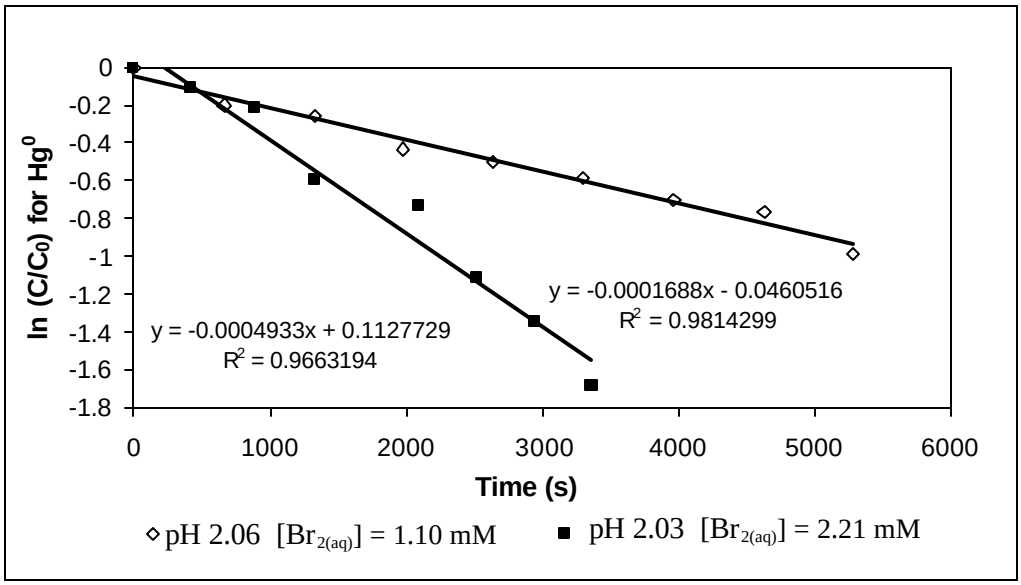

Figure 5.9 The pseudo-first-order plot of the oxidation of Hg^0 by aqueous bromine (Br_2) at pH 2. The slopes of the regressed lines are k_{obs}.

Table 5.2 Summary of Kinetics of Hg^0 + $Br_{2(aq)}$ Reactions Conducted at pH of 2.

pH	n	$[Br_{2(aq)}]_{act}$, mM	$[Hg^0]_{tot}$ µM	$[SO_3^{2-}]$ M	[dithizone] $x10^{-4}$ M	$R^2_{(1st\ order)}$ / $R^2_{(0\ order)}$	k_{obs} s^{-1}	k $M^{-1}s^{-1}$
2.02	5	2.21	0.15	0.067	1.38	0.9255/ 0.8251	0.000398	0.180
2.03	5	1.10	0.13	0.067	1.38	0.9477/ 0.9212	0.000248	0.226
2.03	8	2.21	0.13	0.067	1.38	0.9663/ 0.9745	0.000493	0.223
2.06	9	1.10	0.21	0.036	1.38	0.9814/ 0.9556	0.000169	0.153
								0.196 ± 0.03

n = the number of data points in the pseudo-first-order plot.

5.1.2.2 Hg^0 and HOBr at pH of 6.8

For experiments of aqueous elemental mercury with hypobromous acid at pH of 6.8, the experimental conditions was kept as same as pH of 2, except using a buffer of 12.25 mM sodium dihydrogen phosphate and 7.75 mM sodium phosphate salts to maintain a neutral pH value. Under such conditions, the predominant species is hypobromous acid. Because the dithizone decomposes much more readily under alkaline conditions, a more concentrated dithizone was used at pH of 6.8 and ~ 11.7 with a concentration up to 2.76 x 10^{-4} M.

Figure 5.10 shows the trend of the reaction of aqueous elemental mercury and hypobromous acid at pH of 6.8. It clearly shows the ability of hypobromous acid to oxidize aqueous elemental mercury. Figure 5.11 shows the pseudo-first-order behavior typically found in the kinetic experiments between aqueous elemental

mercury and hypobromous acid (after comparison with R^2 derived from zero or first order kinetic equations in pH 6.8, refer to Table 5.3). The slopes of the plots were taken as the observed rate constants. Table 5.3 shows a compilation of the measured first-order rate constants (k'_{obs}) for the rate of oxidation of elemental mercury in the presence of excess hypobromous acid and the derived second-order rate constants (k). The second-order rate constant of the reaction between aqueous mercury and hypobromous acid is 0.279 ± 0.02 $M^{-1}s^{-1}$.

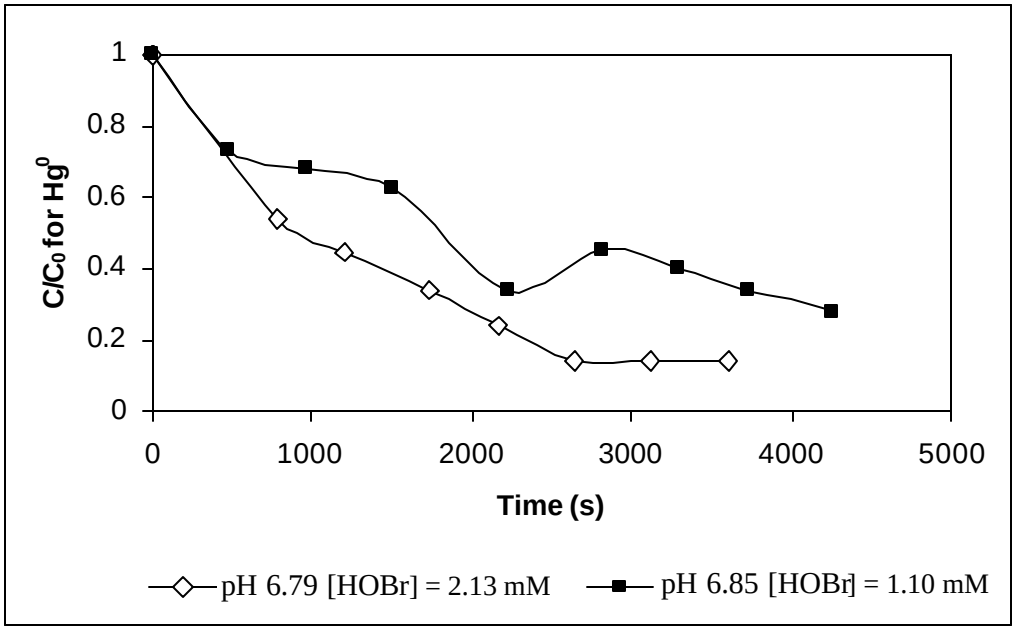

Figure 5.10 Oxidation of aqueous elemental mercury with hypobromous acid (HOBr) at pH 6.8. Initial reactant concentrations: pH 6.79 [Hg^0] = 0.11 µ M, [HOBr] =2.13 mM; pH 6.85 [Hg^0] = 0.09 µ M, [HOBr] = 1.10 mM.

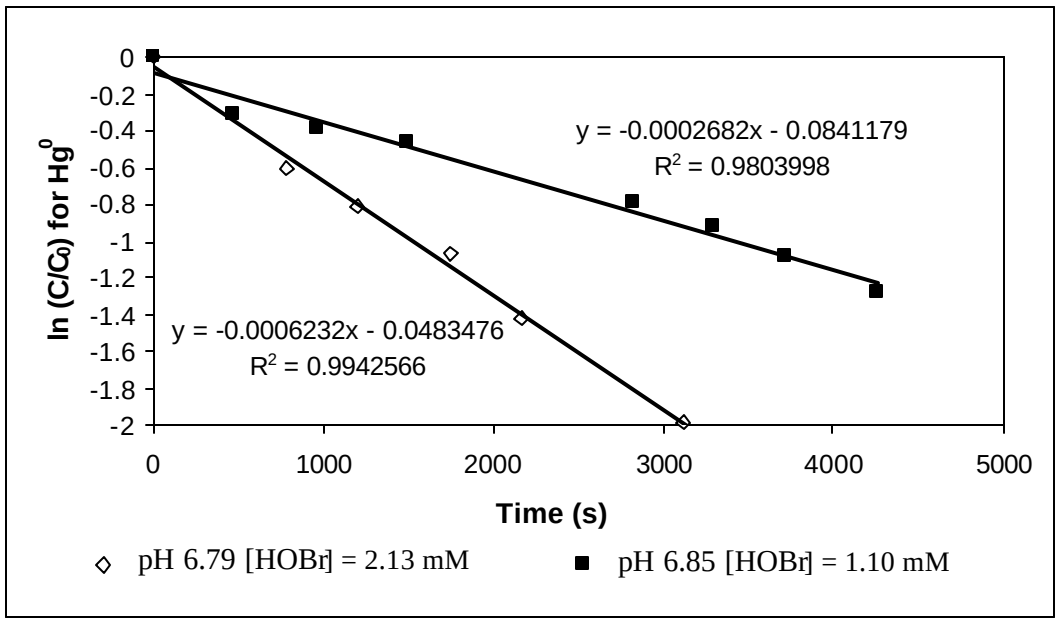

Figure 5.11 The pseudo-first-order plot of the oxidation of Hg^0 by hypobromous acid (HOBr) at pH 6.8. The slopes of the regressed lines are k_{obs}.

Table 5.3 Summary of Kinetics of Hg^0 + HOBr Reactions Conducted at pH of 6.8.

pH	n	$[HOBr]_{act}$, mM	$[Hg^0]_{tot}$ µM	$[SO_3^{2-}]$ M	[dithizone] $x10^{-4}$ M	$R^2_{(1st\ order)}$ / $R^2_{(0\ order)}$	k_{obs} s^{-1}	k $M^{-1}s^{-1}$
6.79	7	2.13	0.113	0.05	2.76	0.9767/ 0.85	0.00066	0.312
6.85	8	1.10	0.09	0.05	2.76	0.9803/ 0.9373	0.00025	0.245
6.86	4	2.14	0.131	0.05	2.76	0.8934/ 0.7173	0.00059	0.274
6.82	6	1.10	0.168	0.033	2.76	0.9495/ 0.9725	0.00032	0.292
6.74	5	2.11	0.100	0.05	2.76	0.9920/ 0.9038	0.00058	0.271
								0.279 ± 0.02

n = the number of data points in the pseudo-first-order plot.

5.2.3 Hg^0 and OBr^- at pH of 11.7

For the experiments conducted at pH of ~ 11.7 between aqueous elemental mercury and hypobromite, 0.01 M sodium hydroxide was used to keep pH constant. Under such conditions, the predominant species is hypobromite. Figure 5.12 shows the elemental mercury concentration fraction profile as a function of time. It is illuminating that the hypobromite also has an oxidation potential sufficiently high to oxidize aqueous elemental mercury. Figure 5.13 shows the pseudo-first-order behavior typically found in kinetic experiments of aqueous elemental mercury and hypobromite. The slopes of the plots were taken as the observed rate constants. Table 5.4 shows a compilation of the measured first-order rate constants (k'_{obs}) for the rate of oxidation of elemental mercury in the presence of excess hypobromite and the derived second-order rate constants (k). The second-order rate constant is 0.273 ± 0.04 $M^{-1}s^{-1}$. Although values of R^2 derived from zero or first order kinetic reaction in pH 12 are almost same value, the pseudo-first order reaction is more preferred, since the zero order reaction is usually rare, most of which are complex reactions occur on the surface.

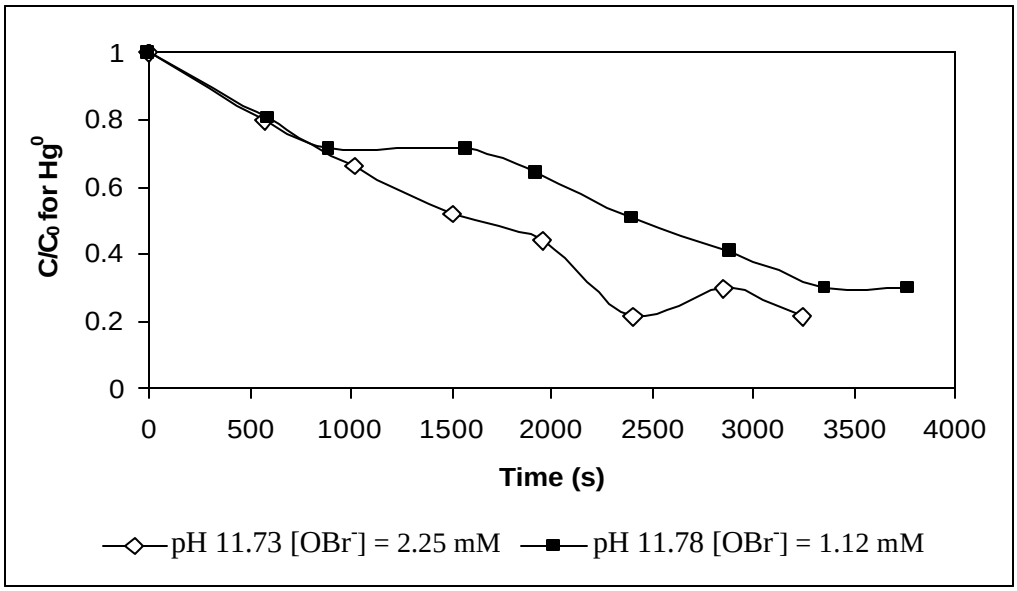

Figure 5.12 Oxidation of aqueous elemental mercury with hypobromite (BrO^-) at pH 11.7. Initial reactant concentrations: pH 11.73 [Hg^0] = 0.14 μ M, [BrO^-] = 2.25 mM; pH 11.78 [Hg^0] = 0.09 μ M, [BrO^-] = 1.12 mM.

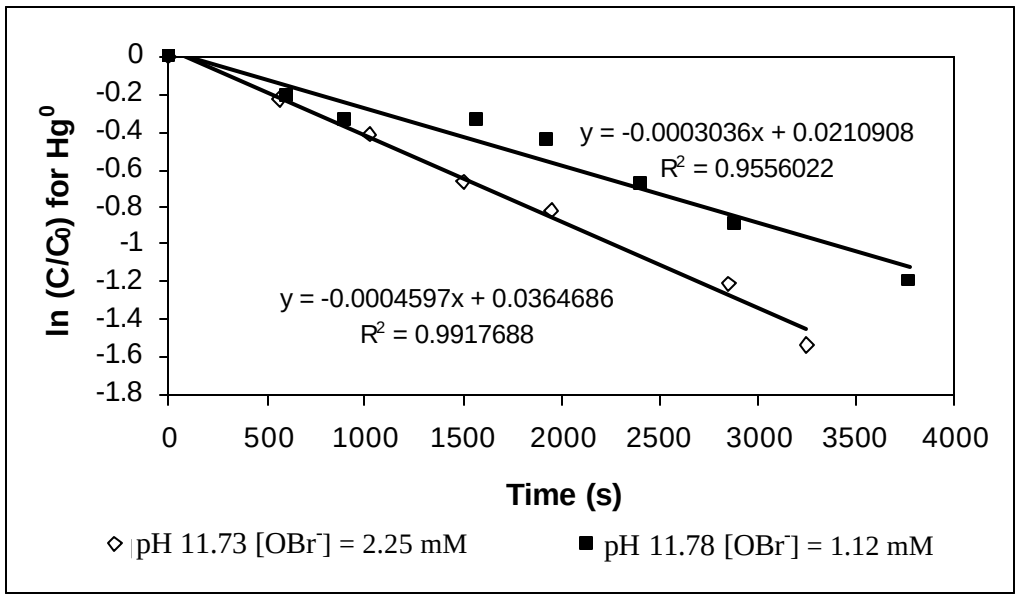

Figure 5.13 The pseudo-first-order plot of the oxidation of Hg^0 by hypobromite (OBr^-) at pH 11.7. The slopes of the regressed lines are k_{obs}.

Table 5.4 Summary of Kinetics of $Hg^0 + OBr^-$ Reactions Conducted at pH of 11.7.

pH	n	$[OBr^-]_{act}$, mM	$[Hg^0]_{tot}$ µM	$[SO_3^{2-}]$ M	[dithizone] x 10^{-4} M	$R^2_{(1st\ order)}$ / $R^2_{(0\ order)}$	k_{obs} s^{-1}	k $M^{-1}s^{-1}$
11.73	7	2.25	0.137	0.066	2.76	0.9918/ 0.9709	0.000460	0.205
11.79	7	1.124	0.096	0.046	2.76	0.9549/ 0.9932	0.000307	0.273
11.78	7	1.124	0.091	0.046	2.76	0.9556/ 0.9639	0.000304	0.270
11.89	6	1.124	0.096	0.014	2.76	0.9773/ 0.954	0.000368	0.327
11.80	6	1.124	0.083	0.046	2.76	0.9258/ 0.9867	0.000328	0.292
								0.273 ± 0.04

n = the number of data points in the pseudo-first-order plot.

Some scattered biases can be detected from above kinetic reaction profiles. Such phenomena may be due to the following factors: firstly, mercury has a high volatility and its vapors can diffuse in or out of the material which used to contain this toxic element, resulting in results that are biased low or high (US EPA, Method 1631, 2001). Secondly, the dithizone method is extreme sensitivity to variations in laboratory conditions, for example, very sensitive to exposing upon light and pH range (Tsubouchi, 1970). Thirdly, the trace amount of mercury was employed in the experiments. But the reactions between elemental mercury and bromine species (bromine, hypobromous acid and hypobromite) are still reproducible.

5.1.3 A COMPARISON OF OXIDATION CAPACITY OF VARIOUS BROMINE SPECIES

A reaction is feasible when the electrode potential of a pair of two half reactions is greater than zero. According to the following electrode potentials of the various bromine species, the oxidation capacity of bromine species arranged by decreasing order is HOBr, Br_2 and OBr^-.

At pH of 2:

$Br_{2(aq)} + Hg(0) \leftrightarrow 2Br^- + Hg^{2+}$

$[Br_{2(aq)}] = 1.125$ mM E = 0.43 V

$[Br_{2(aq)}] = 2.25$ mM E = 0.408 V

At pH of 7:

HOBr + H+ + Hg(0) ←→ Br- + H2O + Hg2+

[HOBr] = 1.125 mM E = 0.696 V

[HOBr] = 2.25 mM E = 0.696 V

At pH of 12:

OBr- + H2O + Hg(0) ←→ Br- + 2OH- + Hg2+

[OBr-] = 1.125 mM E= 0.079 V

[OBr-] = 2.25 mM E= 0.062 V

5.1.4. IMPLICATIONS FOR TROPOSPHERIC MERCURY CHEMISTRY

A sudden mercury increase is observed in the Arctic ecosystem and ice surfaces during the polar sunrise (Poissant, 2001; Lindberg et al., 2002). It is mainly due to reactions of bromine species that probably originate from marine aerosol subsequently deposits on the snow pack (Schroeder et al., 1998; Lu et al., 2001; Poissant, 2001; Lindberg et al., 2002). Bromine species are released from the Arctic sea salt aerosol through an acid-catalyzed activation (Mozurkewich, 1995). In the atmosphere, each aerosol or cloud particle is a closed " reactor chamber"; with its own pH and concentrations of species (Glasow and Dander 2002). And a water droplet can serve as a natural reactor as well as a storage medium for the chemical species involved in the reactions. These airborne chemicals then interact with elemental mercury vapor; ultimately causing the elemental mercury to rapidly oxidize into soluble forms that easily deposit onto snow and ice surfaces. For a better understanding of the global cycle of this toxic metal in the environment, the kinetics of aqueous elemental mercury oxidation by bromine has been studied. The levels of reactive bromine in terrestrial regions are low and its measured concentrations are not available, moreover about 70% of the earth's surface is covered by oceans, a reaction involving bromine released from sea salt aerosols is of potential global importance. The following discussion only concentrates on the typical conditions within the marine boundary layer.

5.1.4.1 Source of Bromine

The most important source of bromine over the ocean is the ocean itself. Sea-salt aerosol particles are produced as sea spray from wind acting on the ocean surface and

the sea-salt aerosol concentrations are strongly dependent on wind velocity (O'Dowd and Smith, 1993; Gong et al., 1997a, 1997b). Inorganic bromine in seawater consists mainly of bromide (Br^-) with a Br^-/Na^+ ratio of 6.25 g/kg. The combustion of biomass or fossil fuels can also serve as a source of bromine compounds (Duce et al., 1983; Maenhaut et al., 1996). Moreover, traffic emissions like the combustion of leaded fuel are considered as an important bromine source (Harrison and Sturges, 1983).

Long term field measurements of sea salt aerosol composition show a decrease of the bromine to sodium ratio of aged sea salt aerosol compared to sea water (Duce et al., 1965; Kritz and Rancher, 1980; Ayers et al., 1998). Bromine deficits can be 30% to 50% on an annual average and maximum monthly mean values of more than 80% are observed. They also show that Br^- deficits were linked to the availability of sulfate acidity in the aerosol, pointing to the importance of acid catalysis in the dehalogenation process (Ayers et al., 1998). High BrO mixing ratios of 0-30 pmol/mol were found during the Arctic polar sunrise (Hausmann and Platt, 1994; Tuckermann et al., 1997). Satellite measurements show large plumes of BrO during the Arctic Spring (Richter et al., 1998; Wagner and Platt, 1998).

When sufficient Br^- is available, the autocatalytic cycles lead to the production of Br_2 and HOBr. This autocatalytic bromine activation cycle proceeds in acidified aerosol, since the reaction consumes H^+ ions. If sufficient NO_x is available, the production of Br_2 and BrCl can be preceded without the need for acid catalysis. These reaction cycles lead to the gradual build-up of total reactive bromine, Br_{tot} (the sum of all gas phase bromine species, except HBr) in the gas phase with maximum values between 8 and 10 pmol/mol. During daylight, the photolysis is the driving force for the net transport of bromine from the aqueous to the gas phase, as the formation of HOBr is dependent on photolytically produced $\cdot HO_2$. The main Br species are HOBr, HBr and

BrO. At night, this is shifted towards Br_2 and BrCl, which are readily photolyzed during daylight. Model-calculated bromide deficits are between 70 and 85 % at 50 m elevation, increasing to more than 90 % in higher model layers due to the lower sea salt aerosol pH in those layers (Glasow and Sander, 2002). The cycle results in the net transfer of Br from the aqueous to the gas phase. The diurnal variation of BrO shows a minimum at around noon and maximum in the morning and evening.

5.1.4.2 Oxidant Capability to Oxidize Mercury

To evaluate the importance of bromine reactions of mercury in light of this kinetic study, eight atmospherically important oxidants are selected and used to estimate the contribution of each to the oxidized mercury in the atmosphere.

The selected oxidants in the aqueous phase are ozone, hypochlorite species, hydroxyl radical, hydrogen peroxide, hypobromous acid, bromine and hypobromite. Table 5.5 shows a summary of the lifetimes of elemental mercury with these oxidants, and presents the capability of these oxidants to contribute to oxidized mercury in the atmosphere. Comparing the concentrations of bromine species present in the atmosphere and the obtained kinetic data relevant to these reactions, the reactions of aqueous bromine species are far too slow to be important atmospheric “sinks” for mercury. Oxidation of mercury in the gas phase by various halogen species is faster than oxidation of mercury in the aqueous phase

5.1.5 MODELING MERCURY CHEMISTRY

Considering the special chemical and physical properties of mercury in the atmosphere, which exists in gas phase, aqueous phase, usually dissolved in cloud or fog droplets, or as the particulate phase, with the forms of primary particulate matter or absorbed on

Table 5.5 Lifetime of Elemental Mercury upon Reactions with Selected Atmospheric Oxidants.

No.	Reaction	Rate Parameter	Typical Range	$K_{H,298}$ ($M\ atm^{-1}$)	Lifetime (s)	Ref.
1	$Hg^0_{(aq)} + O_{3(aq)} + 2H^+$? $Hg^{2+}_{(aq)} + H_2O + O_{2(aq)}$	$4.7 \times 10^7\ M^{-1}s^{-1}$ (1)	30~500 pptv(2)	0.013(3)	3.28E+00	(1) Munthe, 1992 (2) Finlayson-Pitts and Pitts, 1986 (3) Hoffmann and Calver, 1985
2	$Hg^0_{(aq)} + HOCl_{(aq)}$? $Hg^{2+}_{(aq)} + OH^-_{(aq)} + Cl^-$	$2.09 \times 10^6\ M^{-1}s^{-1}$ (1)	Daytime: 5-20 pptv(2.1)	7.61×10^{-2} (3)	3.15E+02 or 9.46E-01	(1) Lin and Pehkonen, 1998 (2.1) Pszenny et al., 1993 (2.2) Impey et al., 1995 (3) Lin and Pehkonen, 1998
3	$Hg^0_{(aq)} + OCl^-_{(aq)} + H^+$? $Hg^{2+}_{(aq)} + OH^-_{(aq)} + Cl^-$	$1.99 \times 10^6\ M^{-1}s^{-1}$ (1)	Nighttime:35 ~70 pptv(2.2)			
4	$Hg^0_{(aq)}$ + ?OH $_{(aq)}$? $Hg^{2+}_{(aq)} + OH^-_{(aq)}$	$2 \times 10^9\ M^{-1}s^{-1}$ (1)	10^{-12} (aq) (2)	25(3)	5.0E+02	(1) Lin and Pehkonen, 1997 (2) Pandis and Seinfeld, 1997 (3) Klaning et al., 1985

No.	Reaction	Rate Parameter	Typical Range	$K_{H,298}$ ($M\ atm^{-1}$)	Lifetime (s)	Ref.
5	$Hg^0_{(aq)} + H_2O_{2(aq)}$? $Hg^{2+}_{(aq)} + HgO_{(s)} + H_2O_{(l)}$	6.0 $M^{-1}s^{-1}$ (1)	200 µM (aq)(2)	$7.4x10^4$(3)	8.33E+02	(1) Munthe and McElroy, 1991 (2) Sakugawa et al., 1990 (3) Lind and Kok, 1986
6	$Hg^0_{(aq)} + HOBr_{(aq)}$? $Hg^{2+}_{(aq)} + OH^-_{(aq)} + Br^-$	0.27 9 $M^{-1}s^{-1}$ (1)	2.8 pptv(2)	1.9 $x10^3$ (3)	6.75E+05	(1) This study (2) Johnson et al., 1999 (3) Blatchley et al., 1992
7	$Hg^0_{(aq)} + Br_{2\ (aq)}$? $Hg^{2+}_{(aq)} + 2Br^-$	0.196 $M^{-1}s^{-1}$ (1)	2.5 pptv(2)	0.68(3)	3.01E+09	(1) This study (2) Glasow et al., 2002 (3) Cotton and Wilkinson, 1972
8	$Hg^0_{(aq)} + OBr^-_{(aq)} + H^+$? $Hg^{2+}_{(aq)} + Br^- + OH^-$	0.273 $M^{-1}s^{-1}$ (1)	4.8 pptv(2)	1.9 $x10^3$ (3)	4.02E+05	1) This study (2) Glasow et al., 2002 (3) Blatchley et al., 1992

Lifetime = $(k\ [oxidant])^{-1}$, k is a second-order rate constant.

existing particles. To better reflect the actual atmospheric conditions, the 3-D comprehensive chemical scheme about evolution of dissolved divalent mercury concentration profile must be considered since dissolved mercury affects the dry and wet deposition. In mercury chemistry model, the gas-phase mercury species needed consideration are Hg(0), $HgCl_2$, $HgBr_2$, $Hg(OH)_2$, and HgO. While, aqueous-phase mercury species are Hg(0), HgO, $HgCl_2$, $HgOH^+$, $Hg(OH)_2$, HgOHCl, $HgSO_3$, $Hg(SO3)_2^{2-}$, Hg^{2+} and $HgBr_2$. Particulate Hg species include HgO and Hg(P), and also cover Hg species adsorbing to soot particles present in cloud droplets (HgO, $HgCl_2$, $HgOH^+$, $Hg(OH)_2$, HgOHCl, $HgSO_3$, $Hg(SO3)_2^{2-}$, $HgBr_2$) and Hg(P) scavenged by cloud droplets (Ryaboshapko et at., 2002) . The identified kinetic reactions about mercury in the gas phase are ozone as well as atomic and molecular halogens (chlorine and bromine) (Hall, 1995; Ariya et al., 2002). However, the oxidants in the aqueous phase are ozone, hydrogen peroxide, hypochlorous acid (HClO & ClO^-), hydroxide radical and bromine species (Munthe, 1991; Munthe and McElory, 1991; Lin and Pehkonen, 1997; Lin and Pehkonen, 1998). The reductants in aqueous phase include sulfite, hydroperoxyl radical, and photoreduction (Munthe, 1991; Xiao et al., 1994; Pehkonen and Lin, 1998). Others parameters needed to be considered are gas-phase diffusion, aqueous-phase diffusion and interfacial transfer, pH, liquid water content, droplet radius and sticking coefficient of Hg0 and so on.

5.2 REACTIONS BETWEEN MERCURY AND IRON IONS

5.2.1 The backward reaction of Hg^0 and Fe^{3+}

Control experiments without ferric iron show that Hg^{2+} concentrations in the reactor in dark do not increase after about 110 minutes and thus a 70 min reaction time was employed (Figure 5.14). The kinetic experiments were performed to investigate the reaction between Hg^0 and Fe^{3+} by using the initial concentration of elemental mercury of 1.1 ~ 2.5 x 10^{-7} M and a ferric iron concentration greater than 3.4 x 10^{-5} M. Figure 5.15 indicates a slow decrease in aqueous elemental mercury when a reaction of Hg^0 and Fe^{3+} is progressing in the dark, but also clearly shows that this reaction proceeds extremely slowly. Under the reaction conditions, the reaction exhibited pseudo-first-order kinetics, as evidenced by the linearity of plots of $\ln[C/C_0]$ for Hg^0 versus time (Figure 5.16). The second-order rate constant, k, can be calculated from the slope. It is found that k is 0.73 ± 0.29 $M^{-1}s^{-1}$ (Table 5.6). The positive value of E (0.051 Volt) under the experimental conditions shows that the oxidation of Hg^0 to Hg^{2+} in the presence of ferric iron is thermodynamically possible. As shown in this study, the reaction between the aqueous ferric iron and aqueous elemental mercury proceeds extremely slowly, rather than very fast and complete, as described in the early 1830's on the oxidation of mercury droplets by ferric iron. Thus, the results obtained with liquid mercury droplets are not relevant to dissolved elemental mercury, and also for natural water systems containing even lower concentrations of dissolved mercury. In natural water systems, although containing high concentrations of iron, since the reaction rate with aqueous elemental mercury is very slow, this pathway cannot be the dominant pathway to transform elemental mercury.

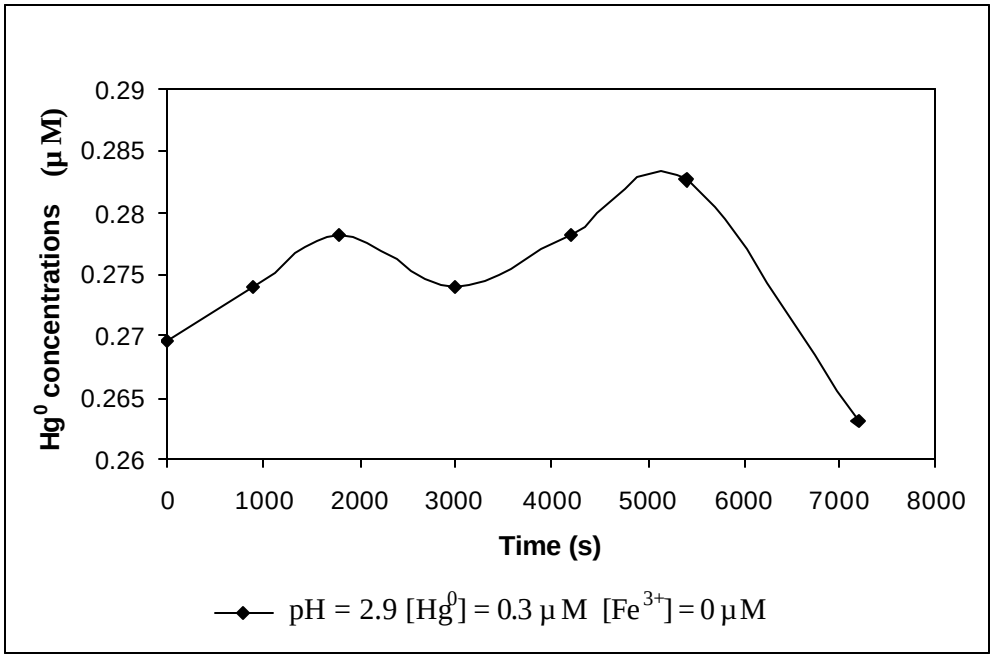

Figure 5.14 A control experiment containing only elemental mercury shows no significant oxidation of elemental mercury during the first 90 minutes.
Conditions: pH 2.9.
Initial concentrations: $[Hg^0]$ = 0.3 µM, $[Fe^{3+}]$ = 0 µM.

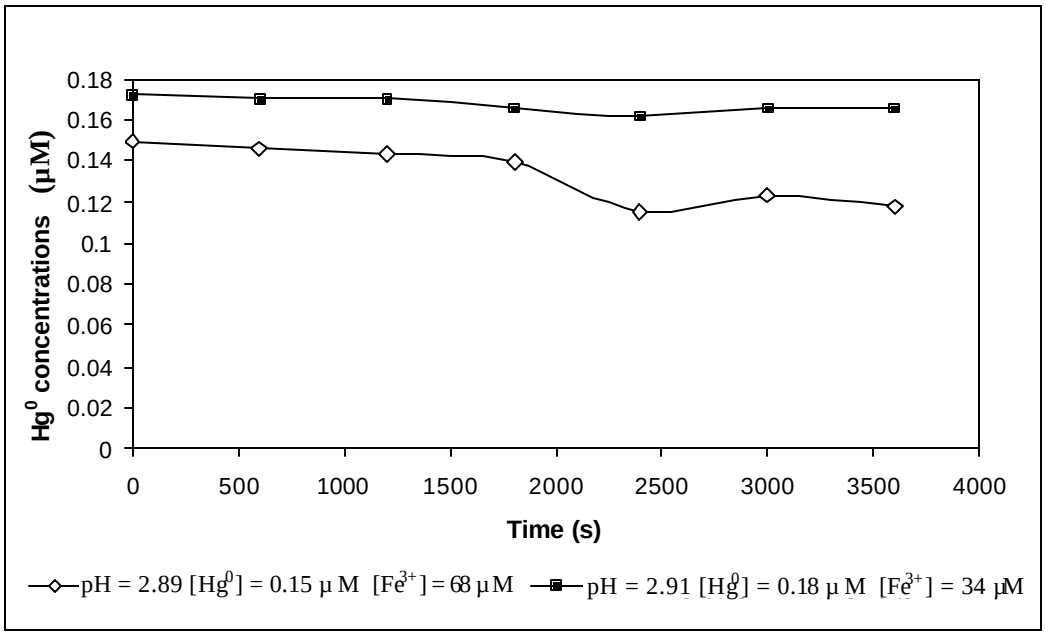

Figure 5.15 Oxidation of aqueous elemental mercury with ferric iron at pH ~2.9.
Initial reactant concentration: pH = 2.89, $[Hg^0]$ = 0.15 µM, $[Fe^{3+}]$ = 68 µM;
pH = 2.91, $[Hg^0]$ = 0.18 µM, $[Fe^{3+}]$ = 34 µM.

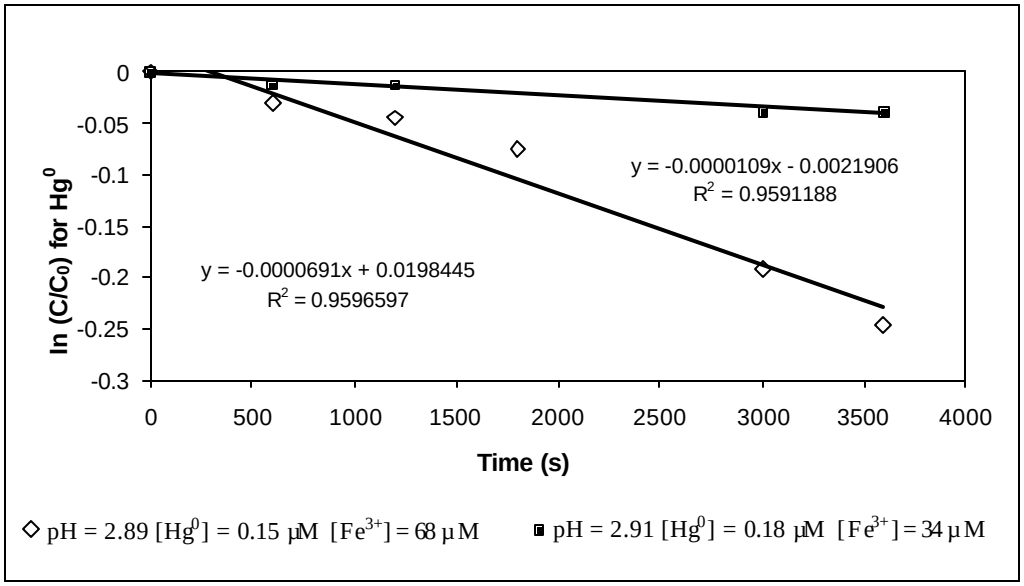

Figure 5.16 The pseudo-first-order plot of the oxidation of Hg^0 by aqueous ferric iron at pH ~ 2.9. The slopes of the regressed lines are k_{obs}.

Table 5.6 Summary of Kinetics of $Hg^0 + Fe^{3+}$ Reactions Conducted at pH of ~2.9.

pH	n	$[Fe^{3+}]$ µM	$[Hg^0]_{tot}$ µM	[Dithizone] M	R^2	k_{obs} s^{-1}	k $M^{-1}s^{-1}$
2.89	4	34	0.25	1.3×10^{-5}	0.936	0.0000258	0.759
2.89	6	68	0.15	1.3×10^{-5}	0.960	0.0000691	1.016
2.91	5	34	0.18	1.3×10^{-5}	0.960	0.0000109	0.321
2.70	5	68	0.182	1.3×10^{-5}	0.920	0.0000548	0.806
							0.73 ± 0.29

n = the number of data points in the pseudo-first-order plot.

5.2.2 The forward reaction of $Hg^{2+} + Fe^{2+}$

All the dark experiments were carried out under the same prescribed conditions for each set of experiment, except for the use of light irradiation and filters. Figure 5.17 indicates a reduction of Hg^{2+} in the dark experiment at pH value of 2.2, 2.5 and 2.9. This decrease is due to the reaction with Fe^{2+} in the dark and/or adsorption onto the wall of the Teflon reactor. On the other hand, Figure 5.18 also shows a decrease in Fe^{2+} in the dark control experiment at pH value of 2.2, 2.5 and 2.9. The loss of ferrous ion may be attributed to the reaction with Hg^{2+}. All the above differences in the concentrations of both Hg^{2+} and Fe^{2+} indicate that the redox reaction in the dark preferred a more acidic environment. Mercury chloride was used throughout the experiments. The presence of the stable complex, $HgCl_{2(aq)}$, under the reaction conditions, and at low pH accelerates the dissolution of this complex and acidity would accelerate the oxidation of Hg^0 to Hg^{2+} (Lindqvist et al., 1984).

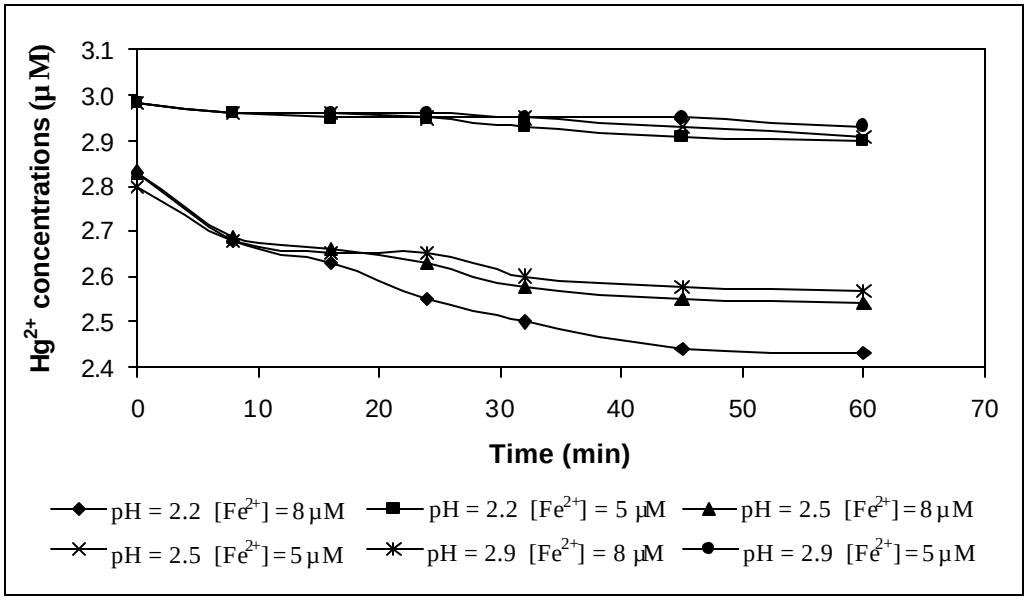

Figure 5.17 The concentration profiles of Hg^{2+} in dark control experiments between Hg^{2+} and Fe^{2+}.
Initial concentrations: $[Hg^{2+}] = 3\ \mu M$, $[Fe^{2+}] = 5$ or $8\ \mu M$.
Conditions: pH 2.2, 2.5 and 2.9.

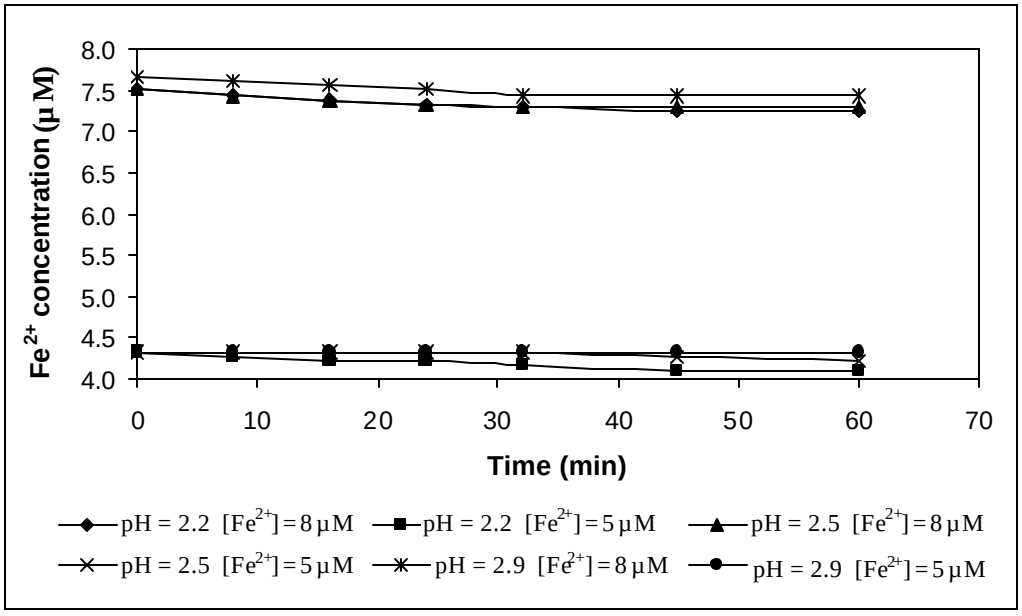

Figure 5.18 The concentration profiles of Fe^{2+} in dark control experiments between Hg^{2+} and Fe^{2+}.
Initial concentrations: $[Hg^{2+}]$ = 3 µM, $[Fe^{2+}]$ = 5 or 8 µM.
Conditions: pH 2.2, 2.5 and 2.9.

5.2.2.1 The Effect of Wavelength

From Figures 5.19, 5.20 and 5.21, it is clearly shown that the dark reaction rate is rather insignificant compared to the reaction with illumination. The photochemical reaction between Hg^{2+} and Fe^{2+} is proceeding much more rapidly when the long pass filter is Model 59423 than 59450. Similarly, the changes in ferrous ion concentrations follow the same trends as those in divalent mercury concentrations (Figure 5.20). Overall, the photochemical reaction would require higher concentrations of ferrous iron in order for the reaction rate to be accelerated. The UV range of sunlight accelerates the reaction.

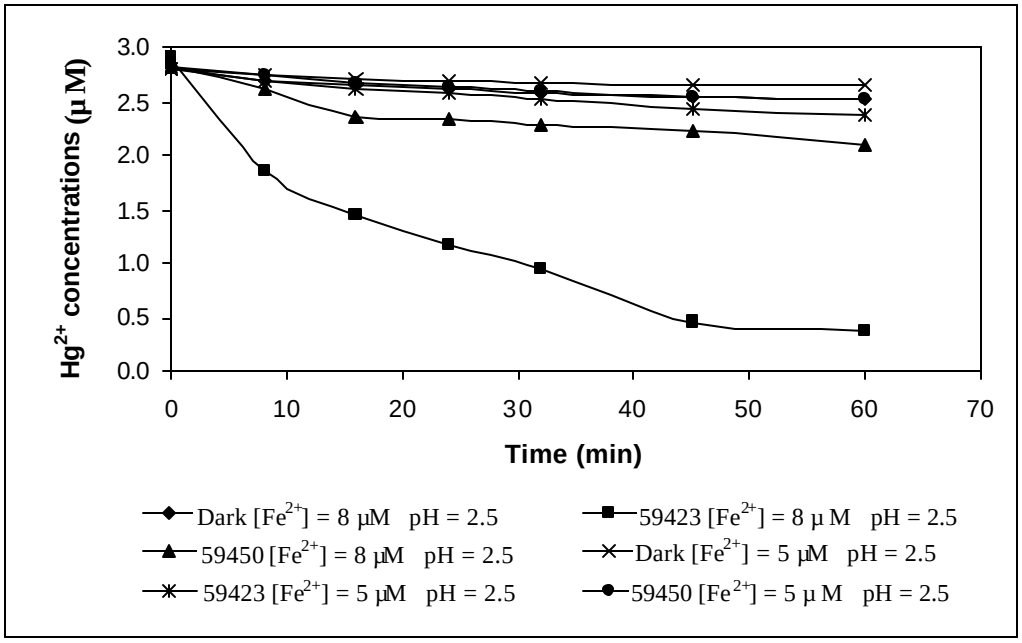

Figure 5.19 The reduction of Hg^{2+} in the presence of Fe^{2+} upon UV light illumination with different bandpass filters.
Conditions: pH 2.5.
Initial concentrations: $[Hg^{2+}]$ = 3 μM, $[Fe^{2+}]$ = 5 or 8 μM.
Bandpass: 59450 (window of transmission from 309 to 800 nm),
59423 (window of transmission from 285 to 800 nm).

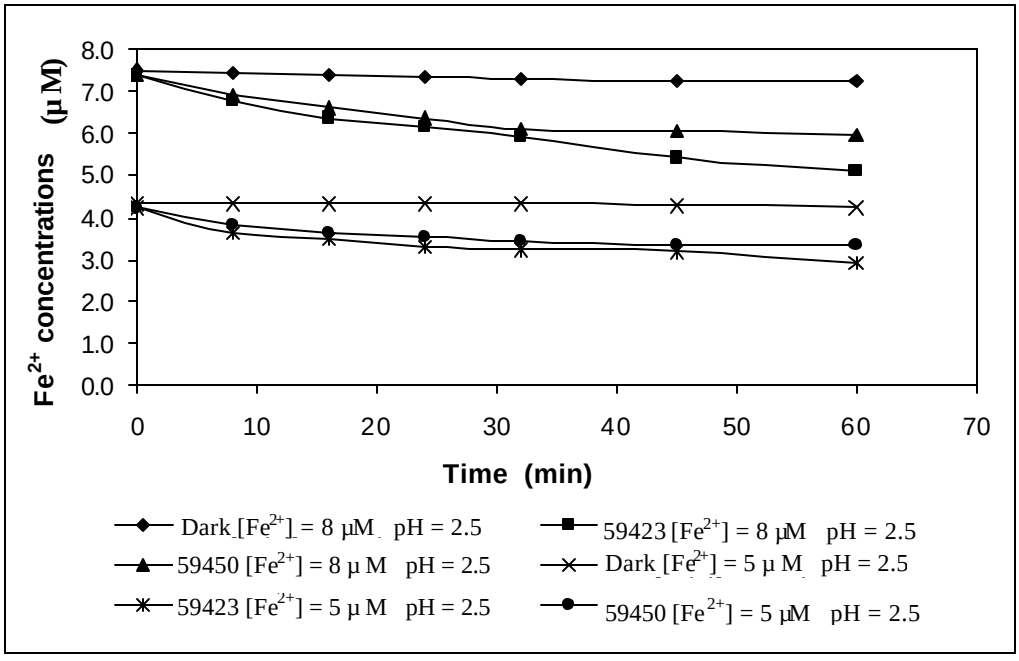

Figure 5.20 The oxidation of Fe^{2+} in the presence of Hg^{2+} upon UV light illumination with different bandpass filters.

Conditions: pH 2.5.
Initial concentrations: [Hg^{2+}] = 3 μ M, [Fe^{2+}] = 5 or 8 μ M.
Bandpass: 59450 (window of transmission from 309 to 800 nm),
59423 (window of transmission from 285 to 800 nm).

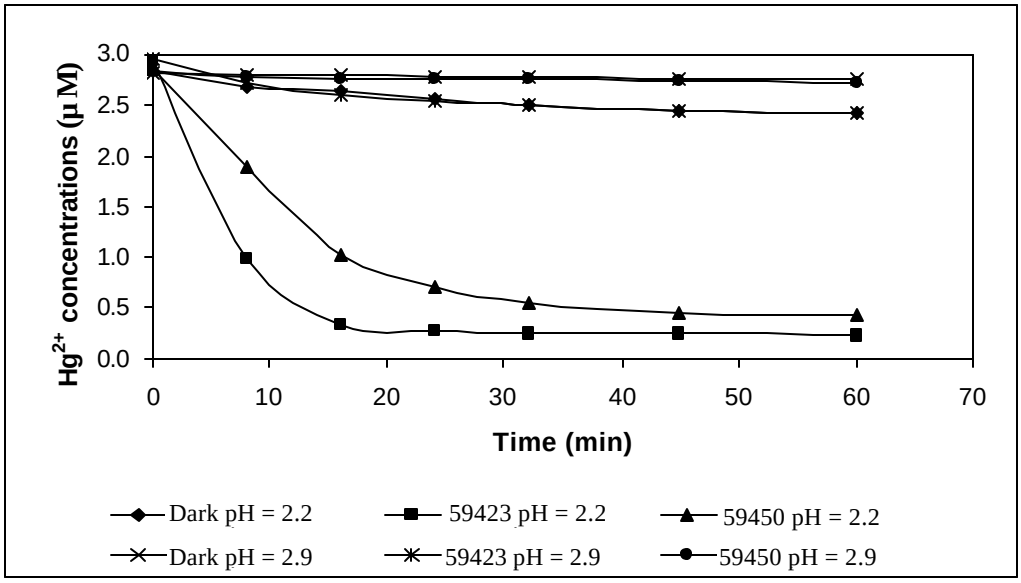

Figure 5.21 The reduction of Hg^{2+} in the presence of Fe^{2+} at different pH values upon light illumination with different bandpass filters.
Conditions: pH 2.2 and 2.9.
Initial concentrations: [Hg^{2+}] = 3 μ M, [Fe^{2+}] = 8 μ M.
Bandpass: 59450 (window of transmission from 309 to 800 nm),
59423 (window of transmission from 285 to 800 nm).

5.2.2.2 Light Intensity

Figure 5.22 shows clearly that the concentration of Hg^{2+} during the light-induced reaction with the use of the neutral density filter, Model 59660, decreases faster than that of Model 59680. It also indicates that the photochemical reaction, regardless of the types of neutral density filters and concentrations of ferrous ions employed, prefers an acidic environment. The changes in ferrous ion concentrations are shown in Figure 5.23.

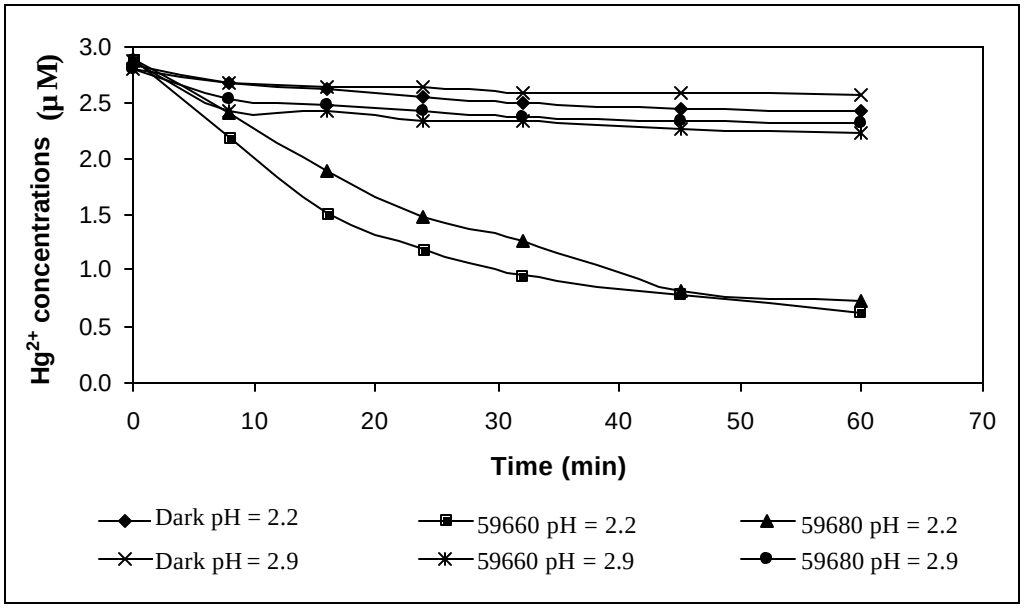

Figure 5.22 The reduction of Hg^{2+} under different light intensity illumination between Hg^{2+} and Fe^{2+}.
Conditions: pH 2.2 and 2.9.
Initial concentrations: [Hg^{2+}] = 3 μ M, [Fe^{2+}] = 8 μ M.
Filters: neutral density filter 59660 (absorbance 0.2) and 59680 (absorbance 0.4).

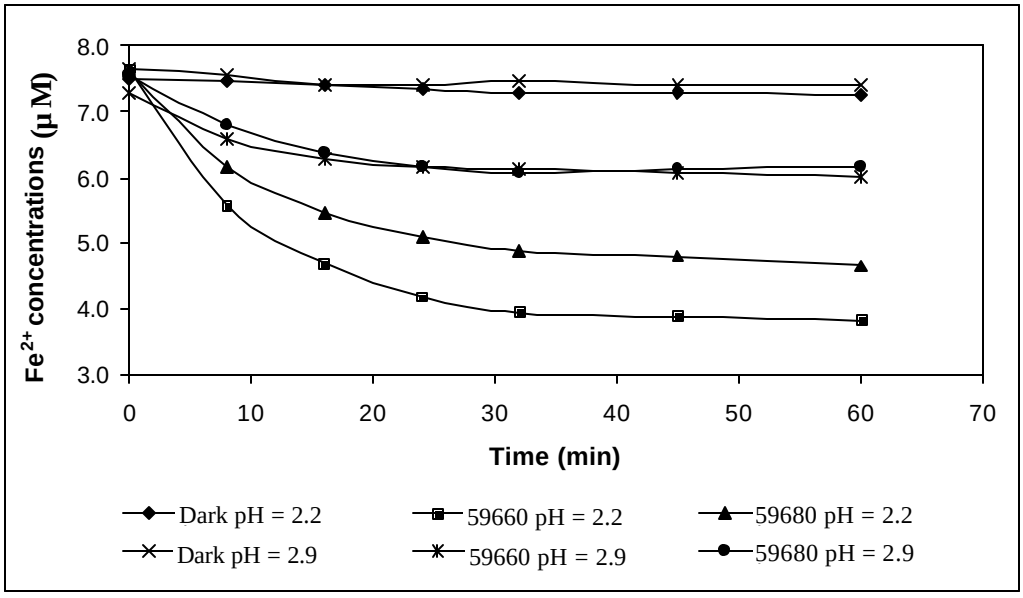

Figure 5.23 The reduction of Fe^{2+} under different light intensity illumination between Hg^{2+} and Fe^{2+}.
Conditions: pH 2.2 and 2.9.
Initial concentrations: [Hg^{2+}] = 3 μ M, [Fe^{2+}] = 8 μ M.
Filters: neutral density filter 59660 (absorbance 0.2) and 59680 (absorbance 0.4).

5.2.3 THE EFFECT OF FLUORIDE ION IN MERCURY DETERMINATION BY THE DITHIZONE METHOD

Sodium fluoride, being a stable complexing agent of ferric iron, was initially used in the reaction system to control free Fe^{3+} concentration. But in such a reaction system, unexpected and unreasonable kinetic reaction curves were obtained. Concentration profiles of Hg^{2+} were not decreasing or increasing in the forward and backward reaction, respectively. Instead, as shown by some experiments in Figures 5.24 and 5.25, Hg^{2+} was fluctuating up and down in a scattered fashion. It was later discovered that fluoride ion is the cause of scattering in the dithizone method. On the other hand, many trial experiments were conducted by altering the concentration of F. As Figures 5.24.and 5.25 depicts, no matter what concentration of F^- was added into the reaction system of backward and/or forward reactions, the scattered data still occurred.

Figure 5.26 shows that the Hg^{2+} calibration curve can have a linear line of regression more than 0.99, but Hg^{2+} with fluoride ion added in, regardless of the F^- concentration, always shows a curve instead of a linear profile. This suggests that the presence of F^- does actually affect the absorbance readings of the Hg^{2+}-dithizone complex in chloroform. But this minor effect can bring such big biases in backward and forward reaction suggest that further investigation need to be carried out to unveil true reaction mechanism of this experiment.

Fluoride ion was initially used in the reaction system as an inhibitor to stop the backward reversible photochemical reaction. But later it become clear that the backward reaction proceeds extremely slowly. Without adding fluoride, the influence of the backward reaction is not too significant.

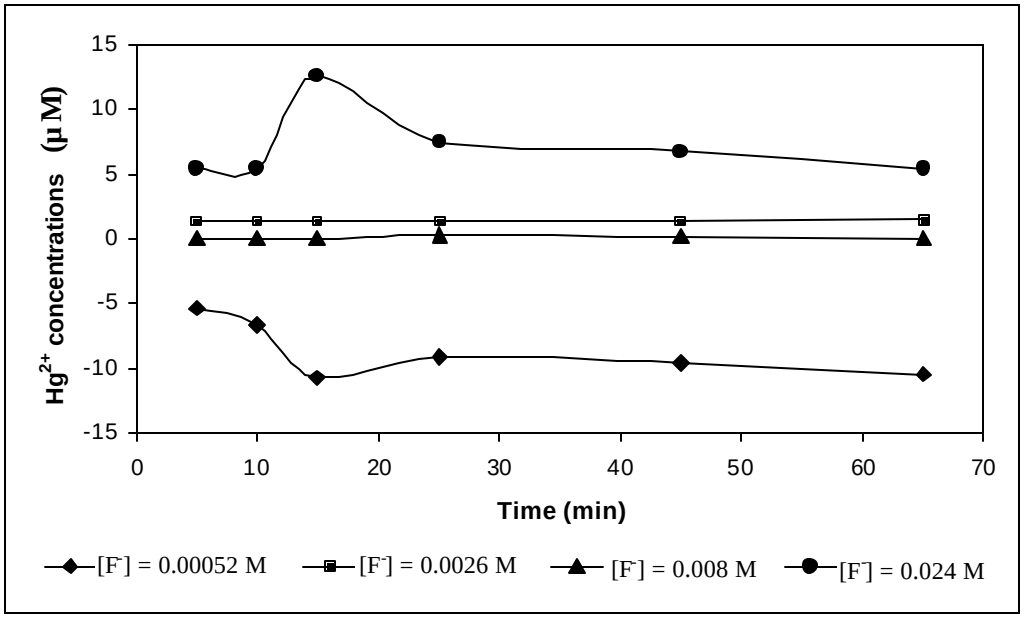

Figure 5.24 Scattered concentrations of divalent mercury appearing in the backward reactions when F^- was added into the reaction system at concentrations from 0.00052 M to 0.024 M.

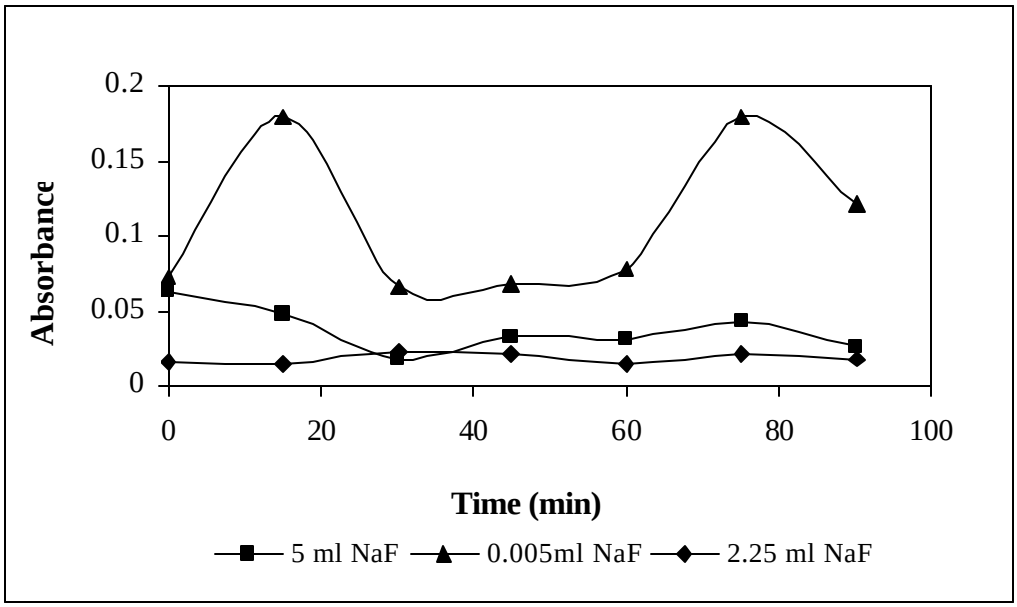

Figure 5.25 Scattered data in the reactions between Hg^{2+} and Fe^{2+} when different NaF was added to the system.

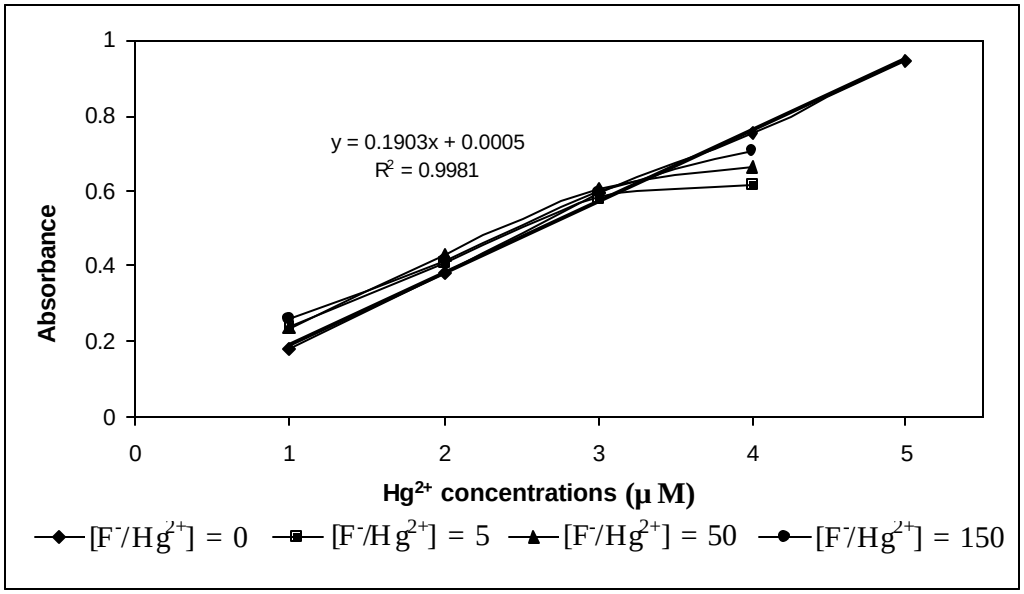

Figure 5.26 The presence of F^- changes the linear relationship between the divalent mercury and the absorbance of the divalent mercury- dithizone complex.

CHAPTER 6

CONCLUSIONS AND FURTHER STUDIES

An extensive kinetic study of the reactions of aqueous mercury with bromine, hypobromous acid, and hypobromite was performed. The second order rate constants at room temperature (20~23°C) for the Hg^0-Br_2, Hg^0- HOBr and Hg^0-OBr^- are determined to be 0.196 ± 0.03 $M^{-1}s^{-1}$, 0.279 ± 0.02 $M^{-1}s^{-1}$ and 0.2733 ± 0.04 $M^{-1}s^{-1}$, respectively.

All the identified oxidants of atmospheric mercury (i.e. O_3, ·OH, H_2O_2, chlorine and bromine) exhibit daily diurnal patterns. Considering the reaction mechanism and the kinetics of aqueous elemental mercury and these oxidants and the concentrations of these species, the kinetic data obtained in this study provide evidence that the rates of the reactions of aqueous elemental mercury with aqueous bromine species are too slow to be important in atmospheric mercury transformation (Table 5.5).

The reduction of divalent mercury and the oxidation of elemental mercury can be achieved by using iron ions. The reduction of divalent mercury is light catalyzed, while the reverse occurs only in the dark.

The reaction in 0.00125 M perchloric acid solution between elemental mercury and ferric iron was found to proceed extremely slowly. The approximate rate constant is ~ 0.73 ± 0.29 $M^{-1}s^{-1}$.

The reaction between divalent mercury and ferrous iron is light-catalyzed. The enhancement of the reduction reaction is due to the following factors: acidic conditions; concentrated ferrous ion environments and the presence of shorter wavelengths (near the UV range of sunlight) and higher light intensity.

Although the Standard Methods does not mention that fluoride interferes in the determination of mercury by the dithizone method, actually no matter what concentrations of F were added into the system, the interference still existed. But the further investigations still need to uncover these variations.

REFERENCES

Adamson, A. W. Electron transfer processes and the oxidation – reduction reaction of hexacyanoferrate (III) iron in aqueous solution. J. Phys. Chem., 56, pp. 858-862. 1952.

Adamson, A. W. Discuss. Faraday Soc., 29, pp. 125. 1960.

Amyot, M., D. R. S. Lean, L. Poissant, M. R. Doyon. Distribution and transformation of elemental mercury in the St. Lawrence River and Lake Ontario, Can. J. Fish. Aquat. Sci., 57, pp. 155-163. 2000.

Anderson, L. D., D. B. Kent and J. A. Davis. Batch experiments characterizing the reduction of Cr(VI) using suboxic material from a mildly reducing sand and gravel aquifer, Environ. Sci. Tech., 28, pp. 178-185. 1994.

Ariya, P. A., A. Khalizov and A. Didas. Reactions of gaseous mercury with atomic and molecular halogens: kinetics, product studies, and atmospheric implications, J. Phys. Chem., A 106, pp. 7310-7320, 2002.

Ayers, G. P., R. W. Gillett, J. M. Cainey and A. L. Dick. Chloride and bromine loss from sea-salt particles in Southern Ocean Air, J. Atmos. Chem., 35, pp. 299-319. 1999.

Batchelor, B., M. Schlautman, I. Wang and R. Wang. Kinetics of chromium (VI) reduction by ferrous iron, Amarillo National Resource Center for Plutonium, Texas Tech. University [Online], ANRCP -1998-13. 1998.
Available: http://www.pu.org/reports/anrc9813.pdf

Beijer, K. and A. Jernelöv. General aspects and specific data on ecological effects of metals in Toxicology of Metals, Vol. III, pp, 201-222. US EPA, PB 208-115. Environmental Protection Agency. 1978.

Berlin, M. Mercury, In: Handbook on the Toxicology of Metals, Vol. II, chapter 15, ed by L. Friberg, pp. 387-435. Amsterdam: Elsevier. 1986.

Bethge, P. O., L. Jonevall-Westöö and L. G. Sillén. Electrometric investigation of equilibria between mercury and halogen ions VI: complexes between Hg^{2+} and Br^{-} and some equilibria involving solid mercury (I) bromide. Acta. Chemica. Scandinavica 2, pp. 828-838, 1948.

Bidstrup, P. L. Clinical symptoms of mercury poisoning in man, J. Biochem., 130, pp.59-60. 1972.

Blatchley, E. R., R. W. Johnson, J. E. Alleman and W. F. McCoy. Effective Henry's law constant for free chlorine and free bromine, Wat. Res., 26, pp. 99-106. 1992.

Bloom, N. S. and W. F. Fitzgerald. Determination of volatile mercury species at the picogram level by low-temperature gas chromatography with cold vapor atomic fluorescence, Anal. Chim. Acta., 208, pp. 151-161, 1988.

Brezonik, P. L. Chemical Kinetics and Process Dynamics in Aquatic Systems. Lewis Publishers: Baca Raton. FL. pp. 643-792. 1994.

Brosset, C. Total airborne mercury and its possible origin, Water, Air, Soil Pollut., 17, pp. 37-50. 1982.

Brosset, C. The behavior of mercury in the physical environment, Water, Air, Soil Pollut., 34, pp. 145-166. 1987.

Buxton, G. V., D. L. Greenstock, W. P. Helman and A. B. Ross. Critical review of rate constants for reactions of hydrated electrons, hydrogen atoms and hydroxyl radicals in aqueous solution, J. Phy, & Chem. Ref. Data., 17(2), pp. 513-780. 1988.

Capozza, K. and P. Fellow. Polar spring arrives, mercury rises - in sky. Environmental News Network [Online]. Available: http://pewfellowships.org/stories/canada/polarspring.html. 2001.

Carpi, A. and S. E. Lindberg. Sunlight-mediated emission of elemental mercury from soil amended with municipal sewage sludge, Environ. Sci. Technol., 31, pp. 2085-2091. 1997.

Clever, H. L., S. A. Johnson and M. E. Derrick. The solubility of mercury and some sparingly soluble mercury salts in water and aqueous electrolyte solution, J. Phys. Chem. Ref. Data., 14, pp. 631-680. 1985.

Cooper, W. J., C. Shao, D. R. S. Lean, A. S. Gordon and F. E. Scully. Factors affecting the distribution of H_2O_2 in surface waters. J. In Environmental Chemistry of Lakes and Reservoirs, ed by L. A. Baker, ACS Symposium Series 237; American Chemical Society: Washington, DC, pp. 391-422. 1994.

Cotton, F. A. and G. Wilkinson. Advanced Inorganic Chemistry. pp. 475, New York: Wiley. 1972.

D'Itri, P. A. and F. M. D'Itri. Mercury Contamination: A Human Tragedy. pp. 311, New York: Wiley-Interscience, 1997.

Duce, R. A., J. W. Winchester and T. W. van Nahi. Iodine, bromine, and chlorine in the Hawaiian marine atmosphere, J. Geophys. Res., 70, pp. 1775-1789. 1965.

Duce, R. A., R. Arimoto, B. J. Ray, C. K. Unni and P. J. Harder. Atmospheric trace elements at Enewetak Atoll, 1, Concentrations, sources, and temporal variability, J. Geophys. Res., 88, pp. 5321-5342. 1983.

Eaton, A. D., L. S. Clesceri and A. E. Greenberg. Standard Methods for the Examination of Water and Wastewater, United Book Press, Inc. 1996.

Ebinghaus, R., R. M. Tripathi, D. W. Wallschläger and S. E. Lindberg. Natural and anthropogenic mercury sources and their impact on the air-surface exchange of mercury on regional and global scales, In Mercury Contaminated Sites,

Characterization, Risk Assessment and Remediation, ed by R. Ebinghaus, R. R. Turner, L. D. de Lacerda, O. Vasiliev and W. Salomons, pp. 4, Berlin: Springer. 1999.

Ellis, D. Environments at risk: case histories of impact assessment, pp.329, Berlin: Springer. 1989.

Expert Panel on Mercury Atmospheric Processes. Mercury atmospheric processes: a synthesis report. Worksh Proc. EPRI/TR-104214, Tampa, Florida, Sep. 1994.

Faust, B. C. In Aquatics and Surface Photochemistry, ed by G. R. Helz, G. ZeppR., D. G. Crosby, Lewis Publishers: Boca Ration, FL., pp. 3-37. 1994.

Fendorf, S. E. and G. C. Li. Kinetics of chromate reduction by ferrous iron, Environ. Sci. Tech., 30, pp. 1614-1617. 1996.

Ferrara, R., B. E. Maserit, H. Edner, P. Pagnarson, S. Svanberg and S. Wallinder. Mercury emissions into the atmosphere from a chlor-alkali complex measured with the lidar technique, Atmos. Environ., 26A, pp. 1253-1258. 1992.

Finlayson-Pitts, B. J. and J. N. Pitts. Atmospheric Chemistry: Fundamentals and experimental techniques. New York: John-Wiley & Sons Inc. 1986.

Fitzgerald, W. F., G. A. Gill and J. P. Kim. An equatorial Pacific Ocean source of atmospheric mercury, Science, 224, pp. 597-599. 1984.

Fitzgerald, W. F. Cycling of mercury between the atmosphere and oceans. In The Role of Air-Sea Exchange in Geochemical cycling, ed by P. Baut-Meanar, pp. 363-408. The Netherlands: NATO Advanced Institute Series, Reidel, Dordrecht. 1986.

Fitzgerald, W. F., R. P. Mason and G. M. Vandal. Atmospheric cycling and air-water exchange of mercury over arid-continental lacustrine regions, Water, Air, Soil Pollut., 56, pp. 745-767. 1991.

Fitzgerald, W. F. Mercury emission from volcanoes. In: 4th Int Conf on Mercury as a global pollutant, ed by R. Ebinghaus, G. Petersen and U. Tümpling. Aug 4-8, 1996, Hamburg, Germany, pp. 87.

Glasow, von R. and R. Sander. Modeling halogen chemistry in the marine boundary layer 1. Cloud-free MBL, J. Geophys. Res., 107, pp. 4341-4356. 2002.

Glass, G. E., J. A. Sorensen, K. W. Schmidt and G. R. Rapp. New source identification of mercury contamination in Great Lakes, Environ. Sci. Tech., 24, pp. 1059-1069. 1990.

Gong, S. L., L. A. Barrie, and J. P. Blanchet. Modeling sea-salt aerosols in the atmosphere, 1, Model development, J. Geophys. Res., 102. pp. 3805-3818. 1997a.

Gong, S. L., L. A. Barrie, J. M. Prospero, D. L. Savoie, G. P. Ayers, J. P. Blanchet and L. Spacek. Modeling sea-salt aerosols in the atmosphere, 2, Atmospheric concentrations and fluxes, J. Geophys. Res., 102. pp. 3819-3830. 1997b.

Hall, B. The gas phase oxidation of elemental mercury by ozone, Water, Air, Soil Pollut., 80, pp. 301-315. 1995.

Harada, M. Minamata disease. organic mercury poisoning caused by ingestion of contaminated fish. In: Adverse effects of foods. Plenum. ed by E. Jallife and D. Jellife, New York: Plenum. 1982.

Harrison, R. M. and W. T. Sturges. The measurement and interpretation of Br/Pb ratios in airborne particles, Atmos. Environ., 17, pp. 311-328. 1983.

Hausmann, M. and U. Platt. Spectroscopic measurement of bromine oxide and ozone in the high Arctic during Polar Sunrise Experiment, J. Geophys. Res., 99, pp. 25,399-25,423. 1994.

Heitanen, S. and L. G. Sillén. Studies on the hydrolysis of metal ions II. The hydrolysis of the mercury (II) ions Hg^{2+}. Acta. Chem. Scand., 6, pp. 747-758. 1952.

Hoffmann, M. R. and J. G. Calvert. Chemical transformation modules for Eulerian acid deposition models. Vol. 2, The aqueous-phase chemistry, Environmental Protection Agency Report No. EPA/600/3-85/017, Research Triangle Park, N. C. 1985.

Impey, G. A., P. B. Shepson., D. R. Hastie, L. A. Barrie and K. G. Anlauf. Measurement of photolyzable chlorine and bromine during the polar sunrise experiment, J. Geophys. Res., 102, pp. 16005-16010. 1995.

Iverfeldt, Å. and O. Lindqvist. Atmospheric oxidation of elemental mercury in the aqueous phase, Atmos. Environ., 20, pp. 1567-1573. 1986.

Iverfeldt, Å. Occurrence and turnover of atmospheric mercury over the Nordic Countries, Water, Air, Soil Pollut., 56, pp. 251-265. 1991.

Jensen, S. and A. Jernelöv. Biological methylation of mercury in aqueous organisms, Nature, 233, pp. 753-754. 1969.

Johnson, D. G., W. A. Traub, K. V. Chance and K. W. Jucks. Detection of HBr and upper limit of HOBr: bromine partitioning in the stratosphere. Smithsonian Astrophysical Observatory. Cambridge, Massachusetts. 1999.

Jugo, S. Retention and distribution of 203 $HgCl_2$ in suckling and adult rats, Health Phys., 30, pp 240-241. 1976.

Klanning, U. K., K. Sehested and J. Holcman. Standard Gibbs free energy of formation of the hydroxyl radical in aqueous solution, J. Phys. Chem., 89, pp. 760-763. 1985.

Kobayashi, T. Oxidation of metallic mercury in aqueous solution by hydrogen peroxide and chlorine, J. Japan Soc. Air. Pollut., 22, pp. 230-236. 1987.

Korringa, P. and P. Hagel. Proceedings International Symposia on Problems on Contamination on Man and His environment by Mercury and Cadmium, Luxembourg, 3-5, July. C.E.C. Luxembourg. 1974.

Kritz, M. and J. Rancher. Circulation of Na, Cl, and Br in the tropical marine atmosphere, J. Geophys. Res., 85, pp. 1633-1639. 1980.

Lacerda, L. C. Global mercury emissions from gold and silver mining, Water, Air, Soil Pollut., 97, pp. 209-221. 1997.

Lalonde, J. D., M. Amyot, A. M. L. Kraepiel and F. M. M. Morel. Photooxidation of Hg(0) in artificial and natural waters. Environ. Sci. Technol., 35, pp. 1367-1372. 2001.

Latimer, W. M. The oxidation states of the elements and their potentials in aqueous solutions, pp. 60, New York: Prentice-Hall. 1939.

Lewin, J. Bromine and its compounds edited by Z. E. Jelles, London Benn. 1966.

Lin, C. J. and S. O. Pehkonen. Aqueous free radical chemistry of mercury in the atmosphere, Atmos. Environ., 32, pp. 2543-2558. 1997.

Lin, C. J. and S. O. Pehkonen. Oxidation of elemental mercury by aqueous chlorine: implications for troposphere mercury chemistry, J. Geophys. Res., 103, pp. 28091-28102. 1998.

Lind, J. A. and G. L. Kok. Henry's law determination for aqueous solution of hydrogen peroxide, methylhydroperoxide and peroxyacetic acid, J. Geophys. Res., 91, pp. 7889-7895. 1986.

Lindberg, S. E., K. H. Kim, T. P. Meyers and J. G. Owens. Micrometeorological gradient approach for quantifying air/surface exchange of mercury vapor: test over contaminated soils, Environ. Sci. Tech., 29, pp. 126-135. 1995.

Lindberg, S. E., and W. J. Stratton. Atmospheric mercury speciation: concentration and behavior of reactive gaseous mercury in ambient air, Environ. Sci. Tech., 32, pp. 49-57, 1998.

Lindberg, S. E., C. Brooks., C. L. Lin, K. J. Scott, M. S. Landis, R. K. Stevens, Goodsite M. and Richter A. Environ. Sci. Tech., 36, pp.1245-1256. 2002.

Lindqvist, O., A. Jernelov, K. Johansson and H. Rodhe, Mercury in the Swedish environment. Global and Local Sources. Report PM 1816. National Swedish Environmental Protection Board, Solna, Sweden. 1984.

Lindqvist, O. and H. Rodhe. Atmospheric mercury - a review, Tellus, 27B, pp. 136-159. 1985.

Lindqvist, O., M. Adstrup; A. Andderson; L. Pringmark; G. Hovsenius; L. Håkanson, Å. Iverfeldt; M. Meili and B. Timm. Mercury in the Swedish Environment-recent

research on causes, consequences and corrective methods. Water, Air. Soil Pollutant., 55, pp. 49-63, 1991.

Lindqvist, O., K. Johansson, M. Aastrup, A. Anderson, L. Bringmark, G. Hovsenius, L. Håkanson, Å Iverfeldt, M. Meili and B. Timm. Mercury in the Swedish environment. Water, Air, Soil Pollut., 55, pp. 261-283. 1991.

Lu, J. Y., W. H. Schroeder, L. A. Barrie, A. Steffen, H. E. Welch, K. Martin, L. Lockhart, R. V. Hunt, G. Boila and A. Richter, Magnification of atmospheric mercury deposition to polar regions in springtime: the link to tropospheric ozone depletion chemistry. Geophys. Res. Lett., 28, pp. 3219-3226. 2001.

Lund-Thompson, E., and Egsgaad. Rate of reaction of dimethylmercury with oxygen atoms in the gas phase, Chem. Phys. Lett., 125, pp. 378-382. 1986.

Maenhaut, W., I Salma, J. Cafmeyer, H. J. Annegarn and M. O. Andreae, Regional atmospheric aerosol composition and sources in the Eastern Transvaal South Africa, and impact of biomass burning, J. Geophys. Res., 101. pp. 23,631-23,650. 1996.

Martell, A. E., R. M. Smith and R. J. Motekaitis. NIST critical stability constants of metal complex database, NIST Standard Reference Data, Gaithersburg, MD. 1993.

Mason, R. P., W. F. Fitzgerald and F. M. M. Morel. The biogeochemical cycling of elemental mercury: anthropogenic influences, Geochim. Cosmochim. Acta, 58, pp. 3191-3198. 1994.

McCAy, L. W. and W. T. Anderson, The reduction of solution of ferric salts with mercury. Princeton University, pp. 2372-2378. 1921.

McElroy, W. J. and J. Munthe. The oxidation of mercury (I) by ozone in acidic aqueous solution, Acta Chemica Scandinavic a, 45, pp. 254-257. 1991.

Mckeown, F. P., I. R. Subramonia and F. S. Rowland. Methylfluoride formation from thermal fluorine-18 reaction with dimethylmercury, J. Phys. Chems., 87, pp. 3972-3975. 1983.

McKnight, D. M., B. A. Kimball and K. E. Bencala. Iron photoreduction and oxidation in an acidic mountain stream, Science, 240, pp. 637-640. 1988.

Meylan, W. M. and P. H. Woward. Computer estimation of the atmospheric gas-phase reaction rate of organic compounds with OH radicals and ozone, Chemosphere 26, PP. 2293-2299. 1993.

Mishima, A. Bitter Sea - the human cost of Minamata disease, pp. 231, Tokyo: Kosei Publishing. 1992.

Mozurkewich, M. Mechanisms for the release of halogens from sea-salt particles by free radicals reactions, J. Geophys. Res., 100, pp. 14,199-14,207. 1995.

Munthe, J., Z. F. Xiao and O. Lindqvist. The aqueous reduction of divalent mercury by sulfite, Water, Air, Soil Pollut., 56, pp. 621-630. 1991.

Munthe, J. and W. J. McElroy. Some aqueous reaction of potential importance in the atmospheric chemistry of mercury, Atmos. Environ., 26A, pp. 553-557. 1991.

Munthe, J. Aqueous oxidation of elemental Hg by O_3, Atmos. Environ., 26A, pp. 1461-1468. 1992.

National Academy of Sciences, Assessment of mercury in the environment. Nati. Acad. of Sci., New York. 1978.

Niki, H., P. S. Maker, C. M. Savage and L. P. Breithbach. A long-path FTIR study of the kinetics and mechanism for the reaction ·OH initiated oxidation of dimethylmercury, J. Phys. Chem., 87, pp. 4878-4981. 1983.

NIOSH (National Institute for Occupational Safety and Health), Registry of toxic effects of chemical substances. National Institute for Occupational Safety and Health. US Department of Health, Education and Welfare. Cincinnati, Ohio. 1978.

Nriagu, J. O. Mechanistic steps in the photoreduction of mercury in natural water, Sci. Tech. Environ., 154, pp. 1-8. 1994.

Nriagu, J. O. and J. M. Pacyna. Quantitative assessment of world-wide contamination of air, water and soils by trace metals, Nature 333, pp. 134-139. 1988.

O'Dowd, C. D. and M. H. Smith. Physicochemical properties of aerosols over the northeast Atlantic: Evidence for wind-speed-related submicron sea-salt aerosol production, J. Geophys. Res., 98. pp. 1137-1149. 1993.

Pandis, S. N. and J. H. Seinfeld. Atmospheric Chemistry and Physics. New York: Wiley-Interscience. 1997.

Pacyna, J. M. Emission inventories of atmospheric mercury from anthropogenic sources. In: Global and regional mercury cycles: sources, fluxes and mass balances. Ed by Baeyens, W., R. Ebinghaus; O. Vasiliev. NATO-ASI Series 2. Environment Vol. 21. pp. 161-178. Kluwer Academic Publishers, Dordrecht, Netherlands. 1996.

Pacyna, J. M. and P. E. Pacyna. Global emissions of mercury to the atmosphere. Emission from anthropogenic sources. A report for the Arctic monitoring and assessment programme (AMMP), Oslo, June 1996.

Pehkonen, S. O. and C. J. Lin. Aqueous photochemistry of divalent mercury with organic acids, J. of Air Waste Management Association, 48, pp. 144-150. 1998.

Pirrone, N., G. J. Keeler and J. O. Nriagu. Regional differences in world-wide emissions of mercury to the atmosphere. Atmos. Environ., 30, pp. 2981-2987. 1996.

Pirrone, N, P. Costa, J. M. Pacyna and R. Ferrara. Mercury emissions to the atmosphere from natural and anthropogenic sources in the Mediterranean region, Atmos. Environ., 35, pp. 2,997-3,006. 2000.

Pleijel, K. and J. Munthe. Modeling the atmospheric mercury cycle - chemistry in fog droplets, Atmos. Environ., 29, pp. 1441-1457. 1995.

Poissant, L. Personal Communication, 2001.

Pszenny, A. A. P., W. C. Keene, D. J. Jacob, S. M. Fan, J. R. Maven, M. P. Zetwo, M. Springer-Young and J. N. Galloway. Evidence of inorganic chlorine gases other than hydrogen chloride in marine surface air, Geophys. Res. Let., 20. pp. 699-702. 1993.

Pyaboshapko, A.; R. Bullock; R. Ebinghaus; I. Ilyin; K. Lohman; J. Munthe; G. Petersen; C. Seigneur and I. Wängberg. Comparison of mercury chemistry models. Atmos. Environ., 36, pp. 3881-3898, 2002.

Raposo, R. R., E. Meléndez-Hevia and M. Spiro. Autocatalytic formation of colloidal mercury in the redox reaction between Hg^{2+} and Fe^{2+} and between Hg_2^{2+} and Fe^{2+}, J. Molecular Catalysis A., 164, pp. 49-59. 2000.

Richter, A., F. Wittrock, M. Eisinger and J. P. Burrows. Some observations of tropospheric BrO in Northern Hemispheric spring and summer 1997, Geophys. Res. Lett., 25, pp. 2683-2686. 1998.

Ross, H. B. and S. J. Vermette. Precipitation. In Trace Elements in Natural Waters, ed by B. Salbu and E. Steinnes, pp. 99-116. Ann. Arbor.: CRC Press. 1995.

Rustam, H. and T. Hamdi. Methylmercury poisoning in Iraq, Brain, 97, pp. 499-510. 1974.

Sakugawa, H., I. R. Kaplan, W. Tasi and Y. Cohen. Atmospheric hydrogen peroxide, Environ. Sci. Tech., 24, pp. 1452-1462. 1990.

Sandell, E. B. Colorimetric determination of traces of metals, 3rd ed., pp. 622-623, USA, Interscience Publishers, 1959.

Schroeder, W. H., G. Yarwood and H. Niki. Transformation processes involving mercury species in the atmosphere --- result from a literature survey, Water, Air, Soil Pollut., 56, pp. 561-667. 1991.

Schroeder, W. H., K. G. Anlauf, L. A. Barrie, J. Y. Lu and A. Steffen. Arctic springtime depletion of mercury, Nature, 394, pp. 331-332. 1998.

Sedlak, D. L. and P. G. Chan. Reduction of hecavalent chromium by ferrous iron, Geochim. Cosmochim. Acta., 61, pp. 2185-2192. 1997.

Seigneur, C., J. Wrobel and E. A. Constantine. A chemical kinetic mechanism for Atmospheric Inorganic Mercury, Environ. Sci. Tech., 28, pp.1589-1597. 1994.

Siegel, S. M. and B. Z. Siegel. First estimate of annual mercury flux at the Kilauea main vent, Nature, 309, pp. 146-147. 1984.

Sillén, L. G. and A. E. Martell. Stability constant of metal ion complexes, pp. 17, London: Special Publication of Chemical Society. 1964.

Slemr, F., W. Seiler and G. Schuster. Latitudinal distribution of mercury over the Atlantic Ocean, J. Geophysical Research, 88, pp. 1159-1166. 1981.

Slemr, F., G. Schuster and W. Seiler. Distribution, speciation and budget of atmospheric mercury, J. Atmos. Chem., 3, pp. 407-434. 1985.

Slemr, F. and E. Langer. Increase in global atmospheric concentrations of mercury inferred for measurements over the Atlantic Ocean, Nature, 355, pp. 434-437. 1992.

Sommar, J., M. Hallquist and E. Ljungström. Rate of reaction between the nitrate radical and dimethylmercury in the gas phase, Chem. Phys. Lett., 257, pp. 434-438. 1996.

Sorensen, J. A., G. E. Glass and K. W. Schmidt. Regional patterns of wet mercury deposition, Environ. Sci. Tech., 28, pp. 2025-2032. 1994.

Stookey, L. L. Ferrozine-a new spectrophotometric reagent for iron, Anal. Chem., 42, pp. 779-781. 1970.

Stumm, W. and J. J. Morgan. Aquatic Chemistry: Chemical Equilibra and Rates in Natural Water. 3rd ed., pp. 726-759. New York: John Wiley & Sons. 1996.

Sukhenko, S. A. and O. F. Vasiliev. A regional mercury budget for Siberia and the role of the region in global cycling of the metal. In: Global and Regional Mercury Cycles: Sources, Fluxes and Mass Balance. NATO-ASI Series 2. Environment vol 21, ed by W. Baeyens, R. Ebinghaus and O. Vasiliev, pp. 123-134. Netherlands. 1996.

Tang, I. N. Thermodynamic and optical properties of mixed-salt aerosols of atmospheric interest, J. Geophys. Res., 102, pp. 1883-1893. 1997.

Tokos, J. J., B. Hall, J. A. Calhoun and E. M. Prestbo. Homogeneous gas-phase reaction of Hg^0 with H_2O_2, O_3, CH_3I, and $(CH_3)_2S$: implications for atmospheric Hg cycle, Atmos. Environ., 32, pp. 823-827. 1998.

Tsubouchi, M. Spectrophotometric determination of trace amounts of mercury (II) by extraction with bindschedler's green, Anal. Chem., 42, pp. 1087- 1088. 1970.

Tuckermann, M., R. Ackermann, C. Golz, H. Lorenzen-Schmidt, T. Senne, J. Stutz, B. Trost, W. Unold, and U. Platt. DOAS-observation of halogen radical-catalysed arctic boundary layer ozone destruction during the ARCTOC-campaigns 1995 and 1996 in Ny-Alesund, Spitsbergen, Tellus, Ser: B, 49, pp. 535-555. 1997.

U. S. Environmental Protection Agency. Health effects assessment of mercury. Environmental Creteria and Assessment Office, Cincinnati Ohio. 1984.

U. S. Environmental Protect Agency. Public health statement for mercury. March 1999.

U. S. Environmental Protect Agency. Mercury in water by oxidation, purge and trap, and cold vapor atomic fluorescence spectrometry, Method 1613, Revision D, EPA-821-R-01-033, October 2001.

Vaughan, P. P. and N. V. Blough. Photochemcial formation of hygroxyl radical by constituents of Natural Waters, Environ. Sci. Tech., 32, pp. 2947-2953. 1998.

Viollier, V., P. W. Inglett, K. Hunter. A. N. Roychoudhury and P. V. Cappellen. The ferrozine method revisited: Fe(II)/Fe(III) determination in natural waters, Appl. Geochem., 15, pp. 785-790. 2000.

Voelker, B. M. and D. L. Sedlak. Iron photoreduction by photoproduced superoxide in seawater, Mar. Chem., 50, pp. 93-102. 1995.

Wagner, T. and U. Platt. Satellite mapping of enhanced BrO concentrations in the troposphere, Nature, 395, pp. 486-490. 1998.

Waite, T. D. and F. M. M. Morel. Photoreductive dissolution of colloidal iron oxides in natural water, Environ. Sci. Tech., 18, pp. 860-868. 1988.

Weast, R. C. CRC Handbook of Chemistry and Physics (70th ed.), CRC Press, Baca Raton, 1989.

WHO (World Health Organization), Guidelines for the assessment of drugs and other chemicals for behavioural teratogenicity. WHO Regional Office for Europe, Copenhagen. 1987.

Wood, J., F. Kennedy and C. Rosen. Synthesis of methlymercury compounds by extracts of a methanogenic bacterium, Nature, 220, pp. 173-174. 1968.

Xiao, Z. F., J. Munthe and O. Lindqvist. Sampling and determination of gaseous and particulate mercury in the atmosphere using gold coated denuders, Water, Air, Soil Pollut., 56, pp. 141-151. 1991a.

Xiao, Z. F., J. Munthe, W. H. Schrodder and O. Lindqvist. Vertical fluxes of volatile mercur y over forest soil and lake surfaces in Sweden, Tellus, 43B, pp. 267-279. 1991b.

Xiao, Z. F., J. Munthe, D. Stromberg and O. Lindqvist. Photochemical behavior of inorganic Hg compounds in aqueous solution. In:. (Eds.), Mercury as a Global Pollutant - Inte gration and Synthesis, ed by C. J. Watras and J. W. Hunkabee. pp. 581-592. New York: Lewis Publishers. 1994.

Zepp, R. G., J. Hoigne and H. Bader. Nitrate induced photooxidation of trace organic chemicals in water, Environ. Sci. Tech., 21, pp. 443-450. 1987.

Zhang, H. and S. E. Lindberg. Processes influencing the emission of mercury from soil: a conceptual model, J. Geophys. Res., 104, pp. 21889-21896. 1999.

Zhang, H. and S. E. Lindberg. Sunlight and Iron (III)-induced photochemical production of dissolved gaseous mercury in freshwater, Environ. Sci. Tech., 35, pp. 928-935. 2001.

Zou, Y. and J. Hoigne. Formation of hydrogen peroxide and depletion of oxalic acid in atmospheric water by photolysis of iron (II)-oxalato complexes, Environ. Sci. Technol., 26, pp. 1014-1022. 1992.